Research Report

Classical and controlled auditory mismatch responses to multiple physical deviances in anaesthetised and conscious mice

Jamie A. O'Reilly[a]* and Bernard A. Conway[b]

[a] College of Biomedical Engineering, Rangsit University, Pathum Thani, Thailand.

[b] Department of Biomedical Engineering, University of Strathclyde, Glasgow, UK.
BC email address: b.a.conway@strath.ac.uk

*Corresponding author: Dr. Jamie Alexander O'Reilly
College of Biomedical Engineering, Rangsit University
52/347 Muang-Ake, Phaholyothin Road,
Pathum Thani 12000, Thailand
t: +66(0)64 783 4785
e: jamie.o@rsu.ac.th

Running title: *Classical and Controlled MMR*

Number of pages: 37

Number of words: 10,061

Number of figures: 6

Abstract

Human mismatch negativity (MMN) is modelled in rodents and other non-human species to examine its underlying neurological mechanisms, primarily described in terms of deviance-detection and adaptation. Using the mouse model, we aim to elucidate subtle dependencies between the mismatch response (MMR) and different physical properties of sound. Epidural field potentials were recorded from urethane-anaesthetised and conscious mice during oddball and many-standards control paradigms with stimuli varying in duration, frequency, intensity, and inter-stimulus interval. Resulting auditory evoked potentials, classical MMR (*oddball* – *standard*), and controlled MMR (*oddball* – *control*) waveforms were analysed. Stimulus duration correlated with stimulus-off response peak latency, whereas frequency, intensity, and inter-stimulus interval correlated with stimulus-on N1 and P1 (conscious only) peak amplitudes. These relationships were instrumental in shaping classical MMR morphology in both anaesthetised and conscious animals, suggesting these waveforms reflect modification of normal auditory processing by different physical properties of sound. Controlled MMR waveforms appeared to exhibit habituation to auditory stimulation over time, which was equally observed in response to oddball and standard stimuli. These findings are inconsistent with the mechanisms thought to underlie human MMN, which currently do not address differences due to specific physical features of sound. Thus, no evidence was found to objectively support the deviance-detection or adaptation hypotheses of MMN in relation to anaesthetised or conscious mice. These findings highlight the potential risk of mischaracterising difference waveform components that are principally influenced by physical sensitivities and habituation of the auditory system.

Introduction

Mismatch negativity (MMN) is a derived electrophysiological signal that is thought to reflect underlying deviance-detection and/or adaptation mechanisms of the auditory system. This signal is a difference measure observed when an evoked response to *oddball* stimulations is compared with the evoked response to repetitive trains of identical *standard* stimuli. Oddball stimuli that deviate from the standard in any discriminable feature of sound are reportedly sufficient to elicit the MMN response (Pakarinen *et al.*, 2007). The auditory-evoked potential (AEP) from the standard is conventionally subtracted from that of the oddball, generating a difference waveform that constitutes the MMN. This may be referred to as the classical approach. Interestingly, MMN is observed from patients in anaesthetised and comatose states (Kane, 1996; Fischer *et al.*, 1999, 2000), suggesting that the mechanisms responsible for its generation do not require consciousness. The prevailing theory is that a mismatch between novel auditory input and a memory-representation, or *predictive model*, of recently experienced auditory inputs triggers updating of this model, thereby subconsciously capturing the attention. This manifests in scalp-recorded EEG as the MMN component (Winkler *et al.*, 1996). This interpretation has remained largely unchanged since its rationale was first proposed (Näätänen *et al.*, 1978), and aligns comfortably within the theory of predictive coding (Wacongne *et al.*, 2012). Some researchers have cited a lack of cellular neurophysiological evidence for this interpretation; instead referring to known properties of sensory neurons, such as stimulus-specific adaptation (SSA), as possible mechanisms of MMN generation (Ulanovsky *et al.*, 2003; Jääskeläinen *et al.*, 2004; May & Tiitinen, 2010). These two propositions, which are referred to as the *memory* and *adaptation* hypotheses of MMN, are not necessarily mutually exclusive, as some researchers

have pointed out (Garrido *et al.*, 2009; Fitzgerald & Todd, 2020); although the extent of their relative contributions is unknown, and a description of the mechanism(s) underlying MMN generation remains incomplete (Ross & Hamm, 2020).

The mechanisms proposed to account for MMN do not sufficiently address differences caused by changes in specific physical features of sound. Mismatch negativity waveforms in response to oddball stimuli varying in duration, frequency, intensity, and other parameters are thought to display unique characteristics; potentially offering clinical utility in measuring associated neurophysiological functions (Näätänen *et al.*, 2004; Pakarinen *et al.*, 2007). For instance, duration MMN deficits are more prominent in the early stages of schizophrenia, whereas frequency deficits, if present, are more likely to emerge later in the disease (Michie *et al.*, 2000; Umbricht & Krljes, 2005; Todd *et al.*, 2008; Atkinson *et al.*, 2012; Erickson *et al.*, 2016). Source localisation studies have indicated that neural generators of duration, frequency, and intensity MMN waveforms are located in separate compartments of the auditory cortex (Frodl-Bauch *et al.*, 1997; Rosburg, 2003; Molholm *et al.*, 2004). Taken together, this evidence suggests that at least partially distinct networks may be responsible for generating duration and frequency MMN. This may logically be extended to other dimensions of auditory deviance. It should also be noted that SSA is almost exclusively studied in response to tone frequency changes, and there is little evidence, to our knowledge, that demonstrates duration- or intensity-specific adaptation; findings have actually suggested that SSA does not occur in response to tone intensity changes (Duque *et al.*, 2016). Thus, we argue that the two most prominent hypotheses of MMN are potentially over-generalized, and therefore insufficient to completely describe the reported observations.

The concept of MMN was initially developed and later established with data from auditory oddball paradigms (Näätänen *et al.*, 1978), and the preponderance of research articles examining MMN are related to this modality. However, change detection is generally thought to be a fundamental sensory process, leading to the application of oddball paradigms incorporating visual (Kojouharova *et al.*, 2019; Male *et al.*, 2020), olfactory (Krauel *et al.*, 1999; Aqrabawi & Kim, 2020) and tactile (Musall *et al.*, 2017; Shen *et al.*, 2018) stimulation. Broadly, these studies tend to confirm that change detection is observed by subtracting neural responses to standards from those of deviants; although the findings presented have not been entirely monolithic. Recently, a well-controlled study of visual MMN identified no evidence of genuine deviance-detection (Male *et al.*, 2020), while a number of previous studies have also shown inconsistencies (Pazo-Alvarez *et al.*, 2003). Considerable challenges are faced while attempting to verify the existence of MMN in each of these modalities; for instance, the requirement for visual attention, and technical requirements for precise control of olfactory and tactile stimulation. As such, the majority of MMN research continues to focus on the auditory domain. The remainder of this article pertains to audition, although the findings presented may be relevant for considering MMN in other sensory systems.

The mouse is an increasingly utilized model species for invasive examination of this potential clinical biomarker, although there are several issues to address concerning their translation. Differences in neuroanatomy and electrophysiology recording techniques can produce substantially different AEP waveforms in terms of latency, polarity, and amplitude of different characteristic peaks. Hence when referring to animal studies the term mismatch response (MMR) has been adopted, opposed to MMN, reflecting a reduced emphasis on latency and polarity (Harms *et al.*, 2016).

The literature is somewhat conflicted regarding the mouse MMR. An initial study highlighted duration MMR in mice as potentially analogous to human duration MMN, although concluded that frequency MMR was not representative of the human frequency MMN (Umbricht *et al.*, 2005). Nevertheless, researchers have generally continued to favour investigation of frequency oddball paradigms in mice, interpreting findings in terms of the existing theoretical framework from human MMN (Ehrlichman *et al.*, 2008, 2009; Featherstone *et al.*, 2013, 2015). Some studies have indicated that strain plays an important role in AEP morphology (Ehlers & Somes, 2002; Siegel *et al.*, 2003), which may account for some variability between results of studies where different mouse strains have been used. Furthermore, differences in electrophysiology recording protocols, oddball paradigms, and interpretation of control waveforms can also obscure direct comparisons of findings from mouse MMR studies. Overall, current evidence for a mouse MMR analogous to the human MMN may be described as promising but inconclusive (Featherstone *et al.*, 2018).

Several different control sequences have been employed in rodent MMR studies. One of the most widely accepted is the *many-standards* control paradigm, in which multiple physically-distinct stimuli, including those used in the oddball paradigm, are presented in pseudo-random order at the same rate as deviants in the oddball paradigm (Schröger & Wolff, 1996; Harms *et al.*, 2014; Wiens *et al.*, 2019). This is designed to control for oddball presentation rate within an irregular sensory-memory trace. Comparison between AEP waveforms produced by the same stimulus in oddball and many-standards paradigms may therefore be used to discriminate between memory- and adaptation-based MMR (Ruusuvirta *et al.*, 2013; Kurkela *et al.*, 2018; Lipponen *et al.*, 2019). In the *flip-flop* control, assignment of standard and oddball stimuli is alternated in two successive presentations of the oddball paradigm

(Harms *et al.*, 2014). The *balanced* oddball paradigm includes two oddball stimuli deviating in the same physical dimension (one increasing and one decreasing) interspersed between standards. This enables a comparison of two separate MMR waveforms by subtracting the standard AEP from two different oddball AEPs. In contrast, the flip-flop control would require four paradigms to examine two difference waveforms relative to the same standard. Given the scope of physical parameters examined, the balanced oddball paradigm and many-standards control were used in the present study, in line with previous studies (Ruusuvirta *et al.*, 2013; Kurkela *et al.*, 2018; Lipponen *et al.*, 2019).

Considering the inclusion of control paradigms, a distinction may be made between classical (*oddball – standard*) and more stringently controlled (*oddball – control*) methods of MMR computation in the preclinical literature. Analysis of these two difference waveforms aims to dissociate between memory and adaptation contributions to MMR generation, and control for different physical levels of stimuli. However, the majority of clinical literature still employs the classical method (Erickson et al. 2016). This raises questions over the translational reliability of rodent MMR for representing human MMN, motivating a closer inspection of both conventional and more rigorously controlled methods of extracting MMR waveforms. We hypothesise that different physical aspects of sound deviance may influence MMR waveforms recorded from the mouse auditory cortex in a feature-specific manner. This study aims to test this hypothesis in urethane-anaesthetised and conscious mice using duration, frequency, intensity, and inter-stimulus-interval (ISI) oddball paradigms. Incorporating a many-standards control paradigm, the presence of any *memory*- or *adaptation*-based generators are assessed, while characterising

the effects of these physical parameters on the resulting mouse AEP and MMR waveforms.

Calculation

Oddball and many-standards paradigms using each feature of sound were presented sequentially, as described in the Materials and Methods. Habituation of the auditory system in response to continued stimulation, characterised by a progressive decline in AEP amplitudes, is a well-established finding in auditory neuroscience (Picton *et al.*, 1976; Ulanovsky *et al.*, 2004). Evoked potentials elicited in consecutive paradigms appeared to demonstrate this phenomenon. Due to this, three waveform comparisons were evaluated, as outlined in Figure 1. *Classical MMR* was generated by subtracting the standard AEP (STD_{OD}) from the oddball AEP (DEV_{OD}). These stimuli were physically distinct but presented during the same paradigm, within a time interval of 10 min. Therefore this waveform may reflect sensory-memory disruption, differential adaptation, and/or physical sensitivity of the auditory system. *Controlled MMR* was evaluated by subtracting physically identical control AEPs (DEV_{CTR}) from their respective oddball AEP (DEV_{OD}); whereas *Controlled Standard* waveforms were computed by subtracting the AEP from standard stimuli presented in oddball and many-standards control paradigms (STD_{CTR}). In both cases, stimuli were physically identical but presented in two different paradigms, occupying consecutive 10 min time intervals, because of the sequential ordering of paradigms. The controlled MMR waveform could reflect oddball-induced sensory memory violation and/or habituation of the auditory response over time; whereas the controlled standard waveform could contain differential adaptation and auditory habituation. This controlled standard differs from previous studies that subtracted the standard AEP from the control AEP based on the presumption of subtracting a more

adapted response from a less adapted response (Harms *et al.*, 2014; Parras *et al.*, 2017). Auditory habituation presented a more plausible explanation for the changes in AEP amplitudes observed between oddball and many-standards control paradigms in the present study; therefore we opted to subtract more habituated waveforms from less habituated waveforms. Reversing the order of subtraction would simply invert the polarity of resulting waveforms. To account for physical differences in the oddball paradigm and habituation differences between oddball and control paradigms, controlled MMR and controlled standard waveforms may be compared. This should reveal whether there is an oddball-induced memory response dissociated from physical sensitivities and auditory habituation; theoretically this could also reflect differential adaptation, although our analyses do not support this.

Materials and Methods

Animals

Laboratory mice (>99.999% C57BL/6J) were used in this study. The anaesthetised group (n = 14) consisted of 9 males and 5 females aged 14 to 17 weeks (mean 15.4). Conscious group (n = 20) consisted of 9 males and 11 females aged 29 to 37 weeks (mean 32.4). These two separate cohorts, which may be considered young and middle-aged adults, respectively, were considered to have sufficient hearing capacity for inclusion in this experiment (Ison *et al.*, 2007). Qualitative between-groups comparisons may be appropriate; although, given that disparity in age could affect hearing, no firm conclusions can be drawn concerning differences between anaesthetised and conscious mouse AEPs. Animal husbandry followed standard guidelines for laboratory mice. All procedures were approved by the Animal Welfare and Ethical Review Board at University of Strathclyde, and performed in accordance with the UK Animals (Scientific Procedures) Act 1986.

Surgery

Urethane-anaesthesia was applied as described elsewhere (Sakata & Harris, 2009), and depth of anaesthesia was confirmed throughout experiments by an absence of normal (tail and toe pinch, eye-blink) reflexes. The conscious experiment group were anaesthetised with isoflurane and oxygen for the duration of aseptic surgery. Skull-screw electrodes (1 mm diameter; Royem Scientific Ltd., Luton, UK) were used to record epidural field potentials. Recording electrodes were implanted bilaterally above the primary auditory cortices (2.2 mm caudal, 3.8 mm lateral, relative to Bregma; Paxinos and Franklin 2004), with a ground electrode implanted above the cerebellum; as previously described (O'Reilly, 2019a). The conscious group were

fitted with a connector (SDL-12-G-10; Samtec, IN, USA), fixed to the skull with dental acrylic, wired to electrodes, providing a conductive path for the amplifiers; after surgery mice recovered for five days before beginning electrophysiological recordings.

Electrophysiology

Mice were placed inside a modified auditory startle reflex chamber (Med Associates Inc., VT, USA) for electrophysiology recording sessions. This consisted of a Faraday cage within an acoustically-controlled cubicle; the inner walls were coated with additional 50 mm, corrugated, sound-absorbing foam (Paulstra Snc., Paris, France). Background noise levels were maintained below 55 dBA sound pressure level (SPL). Anaesthetised animals were positioned facing a loudspeaker (up to 20 kHz frequency response, HK19.5; Harman International, CT, USA), calibrated to the approximate position of their head using a sound meter (A-weighted, Model 33-2055; Radioshack, TX, USA); please see discussion in Supplementary Information concerning sound calibration. Conscious mice were held in a perforated isolation tube (100/44 mm; length/diameter) positioned between front and rear loudspeakers; the average of two calibrations with the sound meter facing either direction was taken in this case. Mice tended to orient themselves longitudinally within the tube, facing either of the speakers. This provided some control over relative sound source location, which is also thought to induce a mismatch negativity response (Perrin *et al.*, 2018), while also reducing movement-related artifacts. The isolation tube had a narrow cut-out along the top, allowing the amplifier tether to enter. Conscious mice were gradually habituated to the test equipment with increasing familiarisation sessions of 5, 15, and 30 min durations on separate training days before beginning recordings. Epidural field potentials were acquired at a sampling rate of 1 kHz and

band-pass filtered from 0.1 to 500 Hz using a tethered amplifier board (Intan Technologies, CA, USA) and stored for post-hoc analysis (open-ephys.org). Stimuli and synchronisation signals were generated in Matlab (Mathworks Inc., MA, USA) and output via a USB i/o device (USB-6255; National Instruments, TX, USA).

Stimulation

Three balanced oddball paradigms, containing both increasing and decreasing deviants, were presented to the anaesthetised group; a separate one for stimuli varying in duration, frequency, and intensity. In addition, the conscious group were presented with an inter-stimulus-interval (ISI) varying oddball paradigm. Inter-stimulus interval is defined as the stimuli offset to onset time. Each oddball paradigm consisted of 800 standards, 100 increasing-oddballs, and 100 decreasing-oddballs; with an ISI of 450 ms (although this was altered in the ISI-varying paradigm). The separation of physical feature variance into different paradigms enabled an examination of each property of sound individually; mitigating potentially confounding effects of multiple-deviances (n.b. non-linear tone frequency loudness perception and sound measurement weighting are addressed in Supplementary Information). An initial sequence of 20 standards was followed by pseudo-random presentation of either increasing or decreasing oddballs, with at least three intervening standards. Standard stimuli were 100 ms, 10 kHz sinusoidal, 80 dBA monophonic tones. Duration oddball stimuli varied by ±50 ms; frequency oddball stimuli varied by ±2.5 kHz (anaesthetised group) or ±2 kHz (conscious group); intensity oddball stimuli varied by ±10 dBA; and ISI oddballs varied by ±50 ms. All stimuli had instantaneous rise and fall times; this caused no distortion of electrical recordings.

Three many-standards control paradigms were presented to the anaesthetised group; the conscious received four, with the addition of an ISI-varying control. These consisted of 10 different stimuli, including the standard and both oddballs from each respective oddball paradigm, presented pseudo-randomly (without repetition) 100 times each, with an ISI of 450 ms (although this was altered in the ISI-varying paradigm). For each version of the many-standards paradigm, the other two physical parameters of stimuli were constant (e.g. in duration-varying paradigms, stimuli frequency and intensity were constant), maintained identical to the standard in the oddball paradigm. The duration many-standards paradigm employed stimuli varying from 50 to 275 ms in 25 ms increments. In the anaesthetised group frequency many-standards stimuli varied from 1.25 to 12.5 kHz in 1.25 kHz increments; in the conscious group these varied from 8 to 12.5 kHz in 500 Hz increments. In the anaesthetised group, intensity many-standards stimuli varied from 60 to 105 dBA in 5 dBA increments; in the conscious group these varied from 70 to 92.5 dBA in 2.5 dBA intervals. The adjustments in stimuli frequency and intensity ranges between groups followed observation of very low-amplitude AEPs in response to stimuli at the lower end of these scales in the anaesthetised group. The ISI many-standards control paradigm incorporated 10 different levels of ISI that varied from 275 to 500 ms in 25 ms increments. All of the stimuli presented in these experiments were designed to be within the normal hearing range of the mice used (Ison et al., 2007).

The anaesthetised group were presented with auditory paradigms immediately following surgery, in a structured protocol lasting approximately 90 min. Duration, frequency and intensity paradigms were presented sequentially, allowing an examination of the influence of deepening anaesthesia and repeated bouts of auditory stimulation on the elicited auditory responses (this analysis is provided in

Supplementary Information). Level of anaesthesia was intermittently monitored by ensuring absence of normal palpebral and corneal reflexes; no reacquisitions of consciousness were observed. The conscious group were presented with counterbalanced duration, frequency, intensity, and ISI-varying paradigms on separate test days, with one intervening non-test day between each; sessions lasted approximately 30 min. In both groups, each feature-specific oddball paradigm was followed by its respective control; e.g. the duration oddball paradigm was followed by the duration many-standards control, facilitating inspection of auditory habituation across paradigms.

Data Analysis

Data were processed with a zero phase-shift low-pass filter with cut-off frequency of 100 Hz. Segments were extracted from −100 to +400 ms about a stimulus-onset timestamp. The pre-stimulus average was subtracted from each segment to perform baseline correction, and trials containing voltages exceeding ±500 μV were removed. Preliminary analysis revealed no significant hemispheric differences between AEPs, comparable with previous findings (Harms *et al.*, 2014). The channel-averaged AEP was therefore computed for each animal, combining left and right electrode data. Only standards immediately preceding oddballs were included in this computation to maintain a relative balance between the number of standard and oddball sweeps contributing to averages.

Significant non-zero amplitudes from difference waveforms were quantified by statistically evaluating every time point. Paired, two-tailed t-tests were performed at every time-point from 0 to 350 ms post-stimulus onset; Benjamini-Yekutieli false discovery rate (FDR) corrections were applied for multiple dependent comparisons

(Benjamini & Yekutieli, 2001), and the alpha value was conventionally set to .05. Regions exceeding the threshold for statistical significance are indicated in the relevant figures.

Auditory evoked potential features quantified from many-standards control waveforms include stimulus-on components, N1 and P1 (conscious animals only), and the stimulus-off response, P_{off}. These were detected over 0 to 30 ms post-onset, 20 to 50 ms post-onset, and 0 to 50 ms post-offset measurement windows, respectively. In the conscious group, stimulus-off potentials from duration many-standards paradigm stimuli were isolated by subtracting the mean AEP from each individual AEP, as described previously (O'Reilly, 2019a). Any effects of stimulus duration, frequency, intensity, or ISI on these AEP features were tested with a one-way, within-subjects, repeated measures analysis of variance, using many-standards paradigm data. In each case, the assumption of sphericity was violated ($p < .05$ in Mauchly's test), therefore Greenhouse-Geisser correction was applied to adjust p-values accordingly; associated epsilon values are reported. Alpha of .05 was used as a threshold for statistical significance. Shaded waveform error-bars represent standard error of the mean (SEM). These analyses were conducted using MNE-Python (Gramfort *et al.*, 2013) and R-studio (RStudio Team, 2016).

Results

Anaesthetised group

The AEP waveforms from duration, frequency, and intensity many-standards paradigms in urethane-anaesthetised mice are plotted in Figure 2a-c, with related peak amplitude and latency measurements provided in Figure 3a-c. The effects of these physical parameters are pronounced. Stimulus duration was directly responsible for P_{off} peak latency [$F_{9,117}$ = 12.93, $p < .0001$; $\varepsilon = .46$]. Stimulus frequency had a significant direct relationship with N1 [$F_{9,117}$ = 27.65, $p < .0001$; $\varepsilon = .29$] and P_{off} [$F_{9,117}$ = 2.97, $p = .029$; $\varepsilon = .43$] peak amplitudes. Stimulus intensity also significantly influenced N1 [$F_{9,117}$ = 27.93, $p < .0001$; $\varepsilon = .20$] and P_{off} [$F_{9,117}$ = 18.25, $p < .0001$; $\varepsilon = .52$] peak amplitudes. Interestingly, lower frequencies (<3.75 kHz) appeared to cause a small positive peak amplitude deflection immediately following the N1 peak. These stimuli are likely nearing the inaudible frequency range for these animals (Ison *et al.*, 2007). In contrast, low intensity 10 kHz stimuli produced a small amplitude N1 peak without being followed by a positive amplitude deflection. These observations led to an adjustment of stimulus frequency ranges in the experiment with conscious mice.

The classical MMR difference waveforms from duration, frequency and intensity oddball paradigms in urethane-anaesthetised mice are plotted in the left half of Figure 4. It is evident from each of these waveforms that the respective physical properties of sound are instrumental in determining MMR morphology. Duration MMR waveforms are caused by P_{off} potentials occurring at different latencies; positive and negative peak amplitudes corresponding to oddball and standard stimuli off-responses, respectively. These produced regions of significant difference, which

are annotated in the difference waveform plot. Frequency MMR waveforms are predominantly influenced by N1 amplitude modulation by stimulus frequency; for this reason, increasing- and decreasing-frequency oddball stimuli produce opposite polarity deflections over the N1 latency range. Similarly, intensity MMR waveforms are generated by N1 and P_{off} amplitude modulation, and increasing- and decreasing-intensity oddballs are observed to produce opposite polarity deflections across N1 and P_{off} latency ranges. Frequency and intensity oddball paradigms did not generate any regions of statistically significant difference within this measurement window; long-latency potentials from frequency and increasing intensity oddball stimuli were observed by applying a double-epoch subtraction method (O'Reilly, 2019b). Controlled MMR waveforms are plotted in the right half of Figure 4. There are marginal differences between oddball and many-standards paradigm AEPs elicited by physically identical stimuli; reflected in both oddball- and standard-minus-control difference waveforms. These minor differences were mainly concentrated at the N1 peak latency, indicative of onset response habituation over time. Peak amplitude measurements from oddball and control paradigm AEPs are plotted in Figure 6a-c.

Conscious group

The AEP waveforms from duration, frequency, intensity and ISI many-standards paradigms in conscious mice are plotted in Figure 2d-g, with relevant peak amplitude data provided in Figure 3d-f. Auditory-evoked potential N1, P1 and P_{off} peaks are observed, with clear effects of each physical parameter. Stimulus duration determined P_{off} peak latency [$F_{9,171} = 8.56$, $p < .0001$; $\varepsilon = .57$], quantified from isolated offset response waveforms (O'Reilly, 2019a). Stimulus frequency had a significant direct relationship with N1 [$F_{9,171} = 5.69$, $p = .00057$; $\varepsilon = .43$] and P1 peak amplitudes [$F_{9,171} = 4.01$, $p = .0069$; $\varepsilon = .41$]. Similarly, stimulus intensity had

statistically significant relationships with N1 [$F_{9,171}$ = 15.63, p < .0001; ε = .32] and P1 [$F_{9,171}$ = 14.08, p < .0001; ε = .36] peak amplitudes. Inter-stimulus interval also had statistically significant direct relationships with both N1 [$F_{9,171}$ = 10.81, p < .0001; ε = .55] and P1 [$F_{9,171}$ = 11.82, p < .0001; ε = .63] peak amplitudes. Peak amplitude measurements from these control paradigm AEPs are plotted on the right side of Figure 3.

Classical MMR waveforms from duration, frequency, intensity and ISI oddball paradigms in conscious mice are plotted in the left half of Figure 5. Prominent negative peak amplitudes in duration MMR waveforms at 125 ms are caused by subtraction of the standard stimulus-off response, and positive peaks at 75 ms and 175 ms are caused by P_{off} of each respective oddball; although these did not achieve the criteria for statistical significance. The longer duration oddball produces greater positive peak amplitude in the MMR, potentially indicating why longer duration oddballs are reported to elicit a greater MMR (Umbricht *et al.*, 2005). Viewing the duration many-standards AEP waveforms (Figure 2d), it may be noted that off-responses from shorter duration stimuli are difficult to distinguish from the larger amplitude deflections. Additionally, offset potentials and difference waveforms in Figure 5a appear to show lower amplitude peaks for the shortest duration stimuli. This is perhaps due to the much larger amplitude N1 and P2 deflections occurring during this latency range. Although, the relationship between offset response peak amplitude and stimulus duration was not found to be significant here. Mismatch responses from frequency, intensity and ISI oddballs exhibit similar waveform morphology. Each of these properties of sound has a direct relationship with N1-P1 peak amplitudes (Figure 2e-g), and accordingly, increasing and decreasing oddball stimuli tended to generate opposite polarity deflections in their respective difference

waveforms. However, it should be noted that there were no statistically significant differences between oddball and standard AEP waveforms from duration, frequency, intensity, or ISI oddball paradigms in conscious mice. An argument may be made that the tests applied were overly conservative, although this approach was selected to avoid bias. Oddball and many-standards control paradigm waveforms are plotted alongside each other in the right hand side of Figure 5. Controlled MMR waveforms highlight changes that similarly influence oddball and standard waveforms, reflected with an alternating polarity trajectory that settles by 100 ms post stimulus onset. These may be interpreted as auditory habituation, or non-stimulus-specific adaptation, accompanying state changes that occur over presentation of subsequent auditory paradigms (illustrated in Figure 1). However, these differences did not exceed the threshold for statistical significance with FDR correction. The lack of substantial difference between controlled MMR and controlled standard waveforms indicates that neither memory- or adaptation-based components were elicited by the oddball condition.

Discussion

Anaesthetised and Conscious States

The discussion begins with a qualitative comparison of AEPs from conscious and anaesthetised groups. Stimulus-on (N1) and stimulus-off (P_{off}) peaks were common to both urethane-anaesthetised and conscious states, whereas P1 and later deflections were only observed from conscious animals. This agrees with previous studies, in which anaesthetised rodents tend to exhibit a less dynamic evoked potential (Nakamura *et al.*, 2011; Harms *et al.*, 2014; Kurkela *et al.*, 2018). One interpretation of this finding is that the neurophysiological mechanisms responsible for generating P1 and subsequent deflections are blocked by anaesthetics. These components may signify aspects of consciousness underpinned by neurotransmitter systems disrupted by urethane; for example, GABA, glycine, N-methyl-D-aspartate (NMDA), α-amino-3-hydroxy-5-methyl-4-isoxazolepropionic acid (AMPA), or acetylcholine (ACh) receptor-mediated signalling (Hara & Harris, 2002). Based on this, it is plausible that alternative anaesthetics with different mechanisms of action to urethane might produce different AEP morphologies. Differences in the AEP between urethane-anaesthetised and conscious mice influence their respective MMR waveforms. This notwithstanding, they also share some similarities. A prominent deflection is present during the N1 latency range in response to frequency, intensity and ISI oddballs from animals in both states. Furthermore, classical duration MMR waveforms from both groups are principally formed by offset responses. It may be argued that these correspondences agree with human MMN, which is also observed in conscious and unconscious states (Kane, 1996; Fischer *et al.*, 1999, 2000; Heinke *et al.*, 2004).

Duration MMR

Auditory stimulus duration is responsible for offset response peak latency (O'Reilly, 2019a). This appears to be instrumental in shaping classical duration MMR difference waveforms; positive peak latency was determined by oddball offset response and negative peak latency determined by the standard offset response (according to the *oddball – standard* computation). This may explain prior findings in conscious mice which found a MMR which varied depending on the duration of standard and oddball stimuli (Umbricht *et al.*, 2005). This also appears to resemble findings from human duration MMN (Takegata *et al.*, 2008; Colin *et al.*, 2009). In a previous study examining duration and frequency deviants in rats, stimulus-off responses were observed from duration-varying stimuli when animals were anaesthetised, but not when they were conscious (Nakamura *et al.*, 2011); for statistical analysis, the investigators averaged together duration and frequency oddball waveforms, and possible influence of the stimulus-off response was not addressed. Combining duration and frequency oddball-evoked waveforms in this way might be inappropriate, given the apparent distinctions between them (Michie *et al.*, 2000; Umbricht & Krljes, 2005; Umbricht *et al.*, 2005; Todd *et al.*, 2008; Erickson *et al.*, 2016). A recent study in urethane-anaesthetised mice observed amplitude modulation to duration deviance, with a shorter oddball producing statistically significant differences relative to the standard (Lipponen *et al.*, 2019). Their study used syllable sound stimuli, which are spectrally more complex than monophonic pure-tones, partially obscuring a comparison of findings; however, it is worth noting that this duration MMR was concluded to be the result of adaptation, given an observed lack of significant difference between oddball and many-standards control waveforms. In the present study, offset potentials were more explicit than previous

studies. For example, a relatively high acoustic signal-to-noise ratio (>25 dB) likely accentuated offset responses, enhancing their visibility from anaesthetised and conscious animals (Baltzell & Billings, 2014; O'Reilly, 2019a). Stimulus duration, sound pressure level, and fall-time also influence cortical activity at sound cessation (Takahashi *et al.*, 2004; Jung *et al.*, 2013). Offset responses are known to occur throughout the auditory system at levels of the brainstem (Henry, 1985), inferior colliculus (Brand *et al.*, 2017), thalamus (He, 2002) and auditory cortex (Qin *et al.*, 2007) in animals/rodents under anaesthesia. These are also observed in EEG recordings from conscious humans (Hillyard & Picton, 1978; Hari *et al.*, 1987), although are only tenuously linked with duration MMN (Jacobsen & Schröger, 2003).

Both onset and offset responses are reactions to abrupt changes in the auditory environment, although their physiological underpinnings in the cortex remain to be fully elucidated (Yamashiro *et al.*, 2009; Kopp-Scheinpflug *et al.*, 2018). Kopp-Scheinpflug et al. (2018) provide a review of offset responses in the auditory system. It has been proposed that auditory stimulus-off responses reflect post-inhibitory rebound following auditory stimulation (Kuwada & Batra, 1999; Phillips *et al.*, 2002; Takahashi *et al.*, 2004). Considering this interpretation, the offset response may reflect the collective activity of inhibitory neurons acting to 'quiet' excitatory neurons in the auditory cortex responding to feedthrough of auditory stimulation from the thalamus. This may be why the onset response peaks before the AEP signal returns towards baseline; then, when auditory stimulation is removed, we observe an overshoot of the inhibitory signal, which is identified here as P_{off}. However, it is argued that both onset and offset responses in the auditory cortex involve separate afferent pathways, suggesting that both are independently driven processes (Scholl *et al.*, 2010). Some research in animals indicates that neurons in the auditory system

are fine-tuned to respond to specific duration stimuli by firing an action potential. Short-, long- and band-duration tuned neurons are reportedly found in the auditory cortex, as are neurons which fire at tone offset (Galazyuk & Feng, 1997; He *et al.*, 1997). In the mouse inferior colliculus, duration-tuning properties and stimulus-off triggered neurons have also been reported (Brand *et al.*, 2017). In the primary auditory cortex of cats, offset-specific neurons have been classified and compared with onset neurons, finding that both are actively triggered (Qin *et al.*, 2007), rather than the off response arising from an inhibition-rebound effect. Implicitly, these effects cannot be disentangled, however, because stimulus offset cannot occur without first having an onset, rendering this debate intractable. Given the large number of neurons in the auditory system, and current limitations of recording techniques, the relationship between onset and offset responses must remain an open question. Nevertheless, the findings of this study directly implicate the stimulus-off response as a key determinant of classical duration MMR in mice. This issue has been discussed previously in the human MMN literature (Jacobsen & Schröger, 2003). Furthering our understanding of this neurophysiological process may be beneficial for interpreting AEP deficits in patients with schizophrenia and genetically susceptible individuals (Shelley *et al.*, 1991; Takegata *et al.*, 2008; Colin *et al.*, 2009). Examination of controlled duration MMR waveforms only illustrated auditory habituation, common to both oddball and standard responses, providing no support for any other mechanism underlying the duration MMR in anaesthetised or conscious mice.

Frequency, Intensity, and ISI MMR

Stimulus frequency, intensity and ISI manipulations similarly influenced N1, P1 and P_{off} features observed from the mouse AEP. This is also true for human N100 and

P200 responses (Picton *et al.*, 1977), potentially suggesting that these features may reflect comparable neurophysiological substrates, preserved across species. These sensitivities caused deflections in each respective classical MMR difference waveform over the latency ranges of these AEP peaks. This was particularly evident from the opposite polarity deflections observed for decreasing versus increasing deviances. The magnitude of these MMR waveforms inherently varies with oddball distance from the standard, which is also true for the human MMN (Pakarinen *et al.*, 2007). However, mouse MMR deflections may be wholly ascribed to the physical characteristics of stimuli themselves, inherently by differences in resulting electrophysiological activity measured from the auditory cortex. This does not clearly reflect sensory-memory or adaptation mechanisms thought to underlie the human MMN, and rather indicates physical modulation of obligatory AEP components. Inspection of controlled standard and controlled MMR waveforms revealed uniform auditory response habituation, without evidence for memory or adaptation components elicited by the oddball condition. Data from rats also suggests that physical properties of stimuli are instrumental in shaping the resulting frequency MMR (Ruusuvirta *et al.*, 2015). This may question the utility of rodents for modelling human MMN. Conversely, the mechanisms underlying human MMN to different physical properties of sound are not completely understood, and may require further clarification to eliminate this as a possibility. Inclusion of appropriate control paradigms in future human studies is therefore highly recommended.

Ascending frequency oddball stimuli in conscious mice produced larger amplitude classical MMR over the P2 latency range. This may reflect non-linearity of the mouse auditory system, which is reported to exhibit tone preference towards ≈14-18 kHz frequencies (Heffner & Heffner, 2007). The findings here may indicate that AEP

amplitudes increase with hearing sensitivity. To examine whether this is true, stimulus frequencies exceeding the range of greatest hearing sensitivity may be applied to test whether a symmetrical decay in amplitude occurs with increasing tone frequencies; although this would require specialist audio equipment, which was not accessible for the present study. An argument may be made that the oddball frequencies were too far removed from the standard (by ±2.5 kHz and ±2 kHz in anaesthetised and conscious groups, respectively), thus influenced by variable hearing thresholds, impeding comparison with human studies. This degree of deviance between standard and oddball stimuli accounts for approximately ±2-2.5% of the mouse hearing range; comparable with relative frequency deviances previously employed in oddball paradigms for human subjects (Michie *et al.*, 2000). The frequencies and deviances used here are also within the usual range, although slightly toward the higher end, applied in rodent MMR studies (Nakamura *et al.*, 2011; Shiramatsu *et al.*, 2013; Harms *et al.*, 2014; Kurkela *et al.*, 2018; Polterovich *et al.*, 2018). Furthermore, the degree of deviance between standard and oddball stimuli has a well-documented effect, which is reportedly to enlarge the MMN amplitude (Shelley *et al.*, 1991; May *et al.*, 1999; Takegata *et al.*, 2008; Colin *et al.*, 2009). This appears to emphasise the fact, because different physical properties of sound have a proportional relationship with AEP amplitudes, that increased separation between standard and oddball frequencies produces greater amplitude difference waveforms.

Effects of stimulus intensity/sound pressure level on the AEP have been studied extensively in both humans and animals. Loudness dependence of the AEP (LDAEP), comparable with observations from this study, has been proposed to reflect serotonergic, dopaminergic and glutamatergic neurotransmission in the

primary auditory cortex (Hegerl & Juckel, 1993; Nathan *et al.*, 2005; O'Neill *et al.*, 2008). This may demonstrate characteristic firing patterns of intensity-tuned, non-monotonic and monotonic, neurons (Phillips & Irvine, 1981). Altered LDAEP is associated with a range of neuropsychiatric diseases, including schizophrenia (Park *et al.*, 2010; Juckel, 2015), which could potentially explain the presence of intensity MMN deficits in patients. Thus, intensity MMR deficits may be due to altered intensity modulation of obligatory AEP components. Inter-stimulus interval modulation of AEP amplitudes has been linked with NMDA receptor signalling, which interestingly is also widely implicated in MMN (Javitt, 2000). To the author's knowledge no neurotransmitter systems have been linked with frequency modulation of the AEP. There is a relative paucity of published studies investigating intensity or ISI MMRs in rodents for comparison, but the data presented here strongly suggests that these are due to physical sensitivities of the auditory system, not memory or adaptation mechanisms. The use of physically identical control waveforms in rodent studies (Nakamura *et al.*, 2011; Harms *et al.*, 2014) does not appear to be widely shared in human MMN studies (Näätänen *et al.*, 2012; Erickson *et al.*, 2016). The majority of research in humans and animal models follows the conventional approach, subtracting standard from oddball AEPs to generate the MMN/MMR waveform (e.g. see the left halves of Figure 4 and Figure 5), which is somewhat disconcerting given that modulation of AEP amplitudes with different physical parameters is a well-established finding in auditory neuroscience.

Auditory Habituation

Sequential ordering of paradigms illustrated the effect of auditory habituation (Picton *et al.*, 1976) on AEP waveforms (e.g. see the right halves of Figure 4 and Figure 5). Amplitudes gradually diminished across paradigms. If this were purely due to SSA,

we would expect to see a differential influence on controlled MMR versus controlled standard responses, because the former represents two conditions with the same presentation rate, while the latter reflects the difference between higher and lower stimulus presentation rates (Nelken, 2014). However, amplitude reductions observed in controlled MMR and controlled standard waveforms were comparable, discounting any overt influence of SSA. Furthermore, lack of substantial differences between controlled MMR and controlled standard waveforms indicates an absence of memory-based component elicited by the oddball. We argue that this approach is more robust than a counterbalanced study design (such as the flip-flop sequence combined with a many-standards control (Harms *et al.*, 2014), which would distribute auditory habituation between subjects across different paradigms. Differential subject habituation rates or minor imbalances in the ordering of paradigms between subjects could lead to considerably uneven distributions of auditory habituation affecting the data. Perhaps this phenomenon contributes towards some of the order-driven effects seen in multi-paradigm MMN studies (Frost *et al.*, 2016; Fitzgerald & Todd, 2020).

Counterbalancing may be taken for granted as a simple procedural control, but when trying to arrange an odd number of paradigms evenly across all subjects, imbalances can easily occur. This may be particularly evident where two sides of the flip-flop oddball paradigm are presented followed by the many-standards control sequence (e.g. Sivarao et al., 2014). This would decrease the probability of finding a significant difference between AEPs from identical stimuli presented in oddball and standard conditions (dismissing the adaptation hypothesis), while increasing the likelihood of observing differences between oddball and control conditions (falsely confirming the memory hypothesis). Few studies we are aware of provide adequate counterbalancing details to fully dissociate this possibility (Harms *et al.*, 2014;

Kurkela *et al.*, 2018; Polterovich *et al.*, 2018). By comparing classic and controlled MMR difference waveforms, it may be possible to dissociate physical sensitivity, auditory habituation, sensory-memory, and adaptation mechanisms. However, examination of these difference waveforms does not provide any strong evidence to objectively support either of the two prevailing hypotheses for MMR generation.

Caveats

The present findings are subject to several limitations. One may be considered the lack of flip-flop control, which is generally used to compare the same stimulus when it is presented as deviant and standard in the oddball paradigm. Besides potentially being affected by state changes between paradigms, this approach seems valid for establishing whether the AEP from a stimulus is influenced by the oddball (e.g. deviance detection) or standard (e.g. repetition suppression) conditions. Nevertheless, the current approach of incorporating a balanced oddball paradigm and many-standards control may be considered equally valid (Ruusuvirta *et al.*, 2013; Kurkela *et al.*, 2018; Lipponen *et al.*, 2019). In addition, incremental differences between stimuli used in many-standards control paradigms were smaller than deviances between stimuli in oddball paradigms. Regarding frequency, there may be concern that this produces greater adaptation of the neural response to stimuli that are presented in the many-standards control. If such a process of cross-stimulation had a prominent effect, we might expect to see evidence of this from stimuli at the extrema of values used; i.e. their responses should be half as "adapted" as the other responses. Analysis of many-standards paradigm waveforms (Figure 2) does not support this. Therefore these caveats do not substantially alter our interpretation of the results.

Conclusion

These findings demonstrate that mismatch response morphology is primarily shaped by physical differences between oddball and standard stimuli. When MMR difference waveforms are computed by the conventional method, these obligatory components can explain all of the observed non-zero amplitudes. This suggests that classical MMR in mice does not reflect a violation of auditory sensory-memory, or adaptation, which are both thought to contribute towards human MMN. Moreover, analysis of controlled MMR and controlled standard waveforms provides no support for either of the existing hypotheses. Overall, this study suggests that difference waveforms in mice are fundamentally influenced by physical sensitivity and habituation of the auditory response. Further work should be cognizant of this interpretation and apply appropriate experimental constraints to confirm the nature of difference waveforms derived from the oddball paradigm.

Acknowledgments

This work was supported in part by funding from the United Kingdom Engineering and Physical Sciences Research Council (EP/F50036X/1).

Author Contributions

JO designed the study, conducted experiments, performed analyses, drafted and revised the manuscript; BC provided supervision and revised the manuscript. Both authors agreed to submission of the final manuscript.

Conflicts of Interest

The authors have no potential conflicts of interest to declare.

Data Availability

The data described in this article are freely available from an online repository (O'Reilly, 2018).

Abbreviations

AEP: auditory evoked potential

DEV_{CTR}: deviant stimulus in the many-standards control paradigm

DEV_{OD}: deviant stimulus in the oddball paradigm

ISI: inter-stimulus interval

MMN: mismatch negativity

MMR: mismatch response

$MMR_{classic}$: conventional MMR, calculated by $DEV_{OD} – STD_{OD}$

$MMR_{control}$: controlled MMR, calculated by $DEV_{OD} – DEV_{CTR}$

N1: first large negative amplitude peak observed in the AEP

P1: first large positive amplitude peak observed in the AEP of conscious mice

P_{off}: positive amplitude peak following stimulus termination

SSA: stimulus-specific adaptation

SPL: sound pressure level

$STD_{control}$: comparison of $STD_{OD} – STD_{CTR}$

STD_{CTR}: standard stimulus in the many-standards control paradigm

STD_{OD}: standard stimulus in the oddball paradigm

References

Aqrabawi, A.J. & Kim, J.C. (2020) Olfactory memory representations are stored in the anterior olfactory nucleus. *Nat. Commun.*, **11**, 1–8.

Atkinson, R.J., Michie, P.T., & Schall, U. (2012) Duration mismatch negativity and P3a in first-episode psychosis and individuals at ultra-high risk of psychosis. *Biol. Psychiatry*, **71**, 98–104.

Baltzell, L.S. & Billings, C.J. (2014) Sensitivity of offset and onset cortical auditory evoked potentials to signals in noise. *Clin. Neurophysiol.*, **125**, 370–380.

Brand, A., Urban, R., & Grothe, B. (2017) Duration Tuning in the Mouse Auditory Midbrain. *J. Neurophysiol.*, **84**, 1790–1799.

Colin, C., Hoonhorst, I., Markessis, E., Radeau, M., de Tourtchaninoff, M., Foucher, A., Collet, G., & Deltenre, P. (2009) Mismatch Negativity (MMN) evoked by sound duration contrasts: An unexpected major effect of deviance direction on amplitudes. *Clin. Neurophysiol.*, **120**, 51–59.

Duque, D., Wang, X., Nieto-Diego, J., Krumbholz, K., & Malmierca, M.S. (2016) Neurons in the inferior colliculus of the rat show stimulus-specific adaptation for frequency, but not for intensity. *Sci. Rep.*, **6**.

Ehlers, C.L. & Somes, C. (2002) Long latency event-related potentials in mice: effects of stimulus characteristics and strain. *Brain Res.*, **957**, 117–128.

Ehrlichman, R.S., Luminais, S.N., White, S.L., Rudnick, N.D., Ma, N., Dow, H.C., Kreibich, A.S., Abel, T., Brodkin, E.S., Hahn, C.G., & Siegel, S.J. (2009) Neuregulin 1 transgenic mice display reduced mismatch negativity, contextual fear conditioning and social interactions. *Brain Res.*, **1294**, 116–127.

Ehrlichman, R.S., Maxwell, C.R., Majumdar, S., & Siegel, S.J. (2008) Deviance-elicited changes in event-related potentials are attenuated by ketamine in mice. *J. Cogn. Neurosci.*, **20**, 1403–1414.

Erickson, M.A., Ruffle, A., & Gold, J.M. (2016) A meta-analysis of mismatch negativity in schizophrenia: From clinical risk to disease specificity and progression. *Biol. Psychiatry*, **79**, 980–987.

Featherstone, R.E., Melnychenko, O., & Siegel, S.J. (2018) Mismatch negativity in preclinical models of schizophrenia. *Schizophr. Res.*, **191**, 35–42.

Featherstone, R.E., Shin, R., Kogan, J.H., Liang, Y., Matsumoto, M., & Siegel, S.J. (2015) Mice with subtle reduction of NMDA NR1 receptor subunit expression have a selective decrease in mismatch negativity: implications for schizophrenia prodromal population. *Neurobiol. Dis.*, **73**, 289–295.

Featherstone, R.E., Tatard-Leitman, V.M., Suh, J.D., Lin, R., Lucki, I., & Siegel, S.J. (2013) Electrophysiological and behavioral responses to ketamine in mice with reduced Akt1 expression. *Psychopharmacology (Berl).*, **227**, 639–649.

Fischer, C., Morlet, D., Bouchet, P., Luaute, J., Jourdan, C., & Salord, F. (1999) Mismatch negativity and late auditory evoked potentials in comatose patients.

Clin. Neurophysiol., **110**, 1601–1610.

Fischer, C., Morlet, D., & Giard, M.-H. (2000) Mismatch negativity and N100 in comatose patients. *Audiol. Neurotol.*, **5**, 192–197.

Fitzgerald, K. & Todd, J. (2020) Making Sense of Mismatch Negativity. *Front. Psychiatry*, **11**, 468.

Frodl-Bauch, T., Kathmann, N., Möller, H.-J., & Hegerl, U. (1997) Dipole localization and test-retest reliability of frequency and duration mismatch negativity generator processes. *Brain Topogr.*, **10**, 3–8.

Frost, J.D., Winkler, I., Provost, A., & Todd, J. (2016) Surprising sequential effects on MMN. *Biol. Psychol.*, **116**, 47–56.

Galazyuk, A. V & Feng, A.S. (1997) Encoding of sound duration by neurons in the auditory cortex of the little brown bat, Myotis lucifugus. *J. Comp. Physiol. - A Sensory, Neural, Behav. Physiol.*, **180**, 301–311.

Garrido, M.I., Kilner, J.M., Stephan, K.E., & Friston, K.J. (2009) The mismatch negativity: A review of underlying mechanisms. *Clin. Neurophysiol.*, **120**, 453–463.

Gramfort, A., Luessi, M., Larson, E., Engemann, D.A., Strohmeier, D., Brodbeck, C., Goj, R., Jas, M., Brooks, T., Parkkonen, L., & Hämäläinen, M. (2013) MEG and EEG data analysis with MNE-Python. *Front. Neurosci.*, **7**, 267.

Hara, K. & Harris, R.A. (2002) The anesthetic mechanism of urethane: the effects on neurotransmitter-gated ion channels. *Anesth. Analg.*, **94**, 313–318.

Hari, R., Pelizzone, M., Mäkelä, J.P., Hällström, J., Leinonen, L., & Lounasmaa, O. V. (1987) Neuromagnetic responses of the human auditory cortex to on- and offsets of noise bursts. *Int. J. Audiol.*, **26**, 31–43.

Harms, L., Fulham, W.R., Todd, J., Budd, T.W., Hunter, M., Meehan, C., Penttonen, M., Schall, U., Zavitsanou, K., Hodgson, D.M., & Michie, P.T. (2014) Mismatch negativity (MMN) in freely-moving rats with several experimental controls. *PLoS One*, **9**.

Harms, L., Michie, P.T., & Näätänen, R. (2016) Criteria for determining whether mismatch responses exist in animal models: Focus on rodents. *Biol. Psychol.*, **116**, 28–35.

He, J. (2002) OFF responses in the auditory thalamus of the guinea pig. *J. Neurophysiol.*, **88**, 2377–2386.

He, J., Hashikawa, T., Ojima, H., & Kinouchi, Y. (1997) Temporal integration and duration tuning in the dorsal zone of cat auditory cortex. *J. Neurosci.*, **17**, 2615–2625.

Heffner, H.E. & Heffner, R.S. (2007) Hearing ranges of laboratory animals. *J. Am. Assoc. Lab. Anim. Sci.*, **46**, 20–22.

Hegerl, U. & Juckel, G. (1993) Intensity dependence of auditory evoked potentials as

an indicator of central serotonergic neurotransmission: A new hypothesis. *Biol. Psychiatry*, **33**, 173–187.

Heinke, W., Kenntner, R., Gunter, T.C., Sammler, D., Olthoff, D., & Koelsch, S. (2004) Sequential effects of increasing propofol sedation on frontal and temporal cortices as indexed by auditory event-related potentials. *Anesthesiol. J. Am. Soc. Anesthesiol.*, **100**, 617–625.

Henry, K.R. (1985) ON and OFF components of the auditory brainstem response have different frequency-and intensity-specific properties. *Hear. Res.*, **18**, 245–251.

Hillyard, S.A. & Picton, T.W. (1978) ON and OFF components in the auditory evoked potential. *Percept. Psychophys.*, **24**, 391–398.

Ison, J.R., Allen, P.D., & O'Neill, W.E. (2007) Age-related hearing loss in C57BL/6J mice has both frequency-specific and non-frequency-specific components that produce a hyperacusis-like exaggeration of the acoustic startle reflex. *J. Assoc. Res. Otolaryngol.*, **8**, 539–550.

Jääskeläinen, I.P., Ahveninen, J., Bonmassar, G., Dale, A.M., Ilmoniemi, R.J., Levänen, S., Lin, F.-H., May, P.J.C., Melcher, J., Stufflebeam, S., & others (2004) Human posterior auditory cortex gates novel sounds to consciousness. *Proc. Natl. Acad. Sci. U. S. A.*, **101**, 6809–6814.

Jacobsen, T. & Schröger, E. (2003) Measuring duration mismatch negativity. *Clin. Neurophysiol.*, **114**, 1133–1143.

Javitt, D.C. (2000) Intracortical mechanisms of mismatch negativity dysfunction in schizophrenia. *Audiol. Neuro-Otology*, **5**, 207–215.

Juckel, G. (2015) Serotonin: From sensory processing to schizophrenia using an electrophysiological method. *Behav. Brain Res.*, **277**, 121–124.

Jung, F., Stephan, K.E., Backes, H., Moran, R., Gramer, M., Kumagai, T., Graf, R., Endepols, H., & Tittgemeyer, M. (2013) Mismatch Responses in the Awake Rat: Evidence from Epidural Recordings of Auditory Cortical Fields. *PLoS One*, **8**, e63203.

Kane, N.M. (1996) Event-related potentials - Neurophysiological tools for predicting emergence and early outcome from traumatic coma. *Intensive Care Med.*, **22**, 39–46.

Kojouharova, P., File, D., Sulykos, I., & Czigler, I. (2019) Visual mismatch negativity and stimulus-specific adaptation: the role of stimulus complexity. *Exp. Brain Res.*, **237**, 1179–1194.

Kopp-Scheinpflug, C., Sinclair, J.L., & Linden, J.F. (2018) When Sound Stops: Offset Responses in the Auditory System. *Trends Neurosci.*, **41**, 712–728.

Krauel, K., Schott, P., Sojka, B., Pause, B.M., & Ferstl, R. (1999) Is there a mismatch negativity analogue in the olfactory event-related potential? *J. Psychophysiol.*, **13**, 49–55.

Kurkela, J.L.O., Lipponen, A., Kyläheiko, I., & Astikainen, P. (2018) Electrophysiological evidence of memory-based detection of auditory regularity violations in anesthetized mice. *Sci. Rep.*, **8**, 3027.

Kuwada, S. & Batra, R. (1999) Coding of sound envelopes by inhibitory rebound in neurons of the superior olivary complex in the unanesthetized rabbit. *J. Neurosci.*, **19**, 2273–2287.

Lipponen, A., Kurkela, J.L.O., Kyläheiko, I., Hölttä, S., Ruusuvirta, T., Hämäläinen, J.A., & Astikainen, P. (2019) Auditory-evoked potentials to changes in sound duration in urethane-anaesthetized mice. *Eur. J. Neurosci.*, **50**, 1911–1919.

Male, A.G., O'Shea, R.P., Schröger, E., Müller, D., Roeber, U., & Widmann, A. (2020) The quest for the genuine visual mismatch negativity (vMMN): Event-related potential indications of deviance detection for low-level visual features. *Psychophysiology*, **57**.

May, P.J.C. & Tiitinen, H. (2010) Mismatch negativity (MMN), the deviance-elicited auditory deflection, explained. *Psychophysiology*, **47**, 66–122.

May, P.J.C., Tiitinen, H., Ilmoniemi, R.J., Nyman, G., Taylor, J.G., & Näätänen, R. (1999) Frequency Change Detection in Human Auditory Cortex. *J. Comput. Neurosci.*, **6**, 99–120.

Michie, P.T., Budd, T.W., Todd, J., Rock, D., Wichmann, H., Box, J., & Jablensky, A. V. (2000) Duration and frequency mismatch negativity in schizophrenia. *Clin. Neurophysiol.*, **111**, 1054–1065.

Molholm, S., Martinez, A., Ritter, W., Javitt, D.C., & Foxe, J.J. (2004) The neural circuitry of pre-attentive auditory change-detection: an fMRI study of pitch and duration mismatch negativity generators. *Cereb. Cortex*, **15**, 545–551.

Musall, S., Haiss, F., Weber, B., & Behrens, W. von der (2017) Deviant processing in the primary somatosensory cortex. *Cereb. Cortex*, **27**, 863–876.

Näätänen, R., Gaillard, A.W.K., & Mäntysalo, S. (1978) Early selective-attention effect on evoked potential reinterpreted. *Acta Psychol. (Amst).*, **42**, 313–329.

Näätänen, R., Kujala, T., Escera, C., Baldeweg, T., Kreegipuu, K., Carlson, S., & Ponton, C. (2012) The mismatch negativity (MMN) - A unique window to disturbed central auditory processing in ageing and different clinical conditions. *Clin. Neurophysiol.*, **123**, 424–458.

Näätänen, R., Pakarinen, S., Rinne, T., & Takegata, R. (2004) The mismatch negativity (MMN): Towards the optimal paradigm. *Clin. Neurophysiol.*, **115**, 140–144.

Nakamura, T., Michie, P.T., Fulham, W.R., Todd, J., Budd, T.W., Schall, U., Hunter, M., & Hodgson, D.M. (2011) Epidural auditory event-related potentials in the rat to frequency and duration deviants: Evidence of mismatch negativity? *Front. Psychol.*, **2**, 367.

Nathan, P.J., O'Neill, B., Croft, R.J., Gallinat, J., Hellweg, R., & Lang, U.E. (2005) Is the loudness dependence of the auditory evoked potential a sensitive and

selective in vivo marker of central serotonergic function? (multiple letters). *Neuropsychopharmacology*, **30**, 1584–1587.

Nelken, I. (2014) Stimulus-specific adaptation and deviance detection in the auditory system: experiments and models. *Biol. Cybern.*, **108**, 655–663.

O'Neill, B. V., Croft, R.J., & Nathan, P.J. (2008) The loudness dependence of the auditory evoked potential (LDAEP) as an in vivo biomarker of central serotonergic function in humans: rationale, evaluation and review of findings. *Hum. Psychopharmacol. Clin. Exp.*, **23**, 355–370.

O'Reilly, J.A. (2018) Oddball and many-standards paradigm auditory-evoked potential data from laboratory mice. *Mendeley Data*, **v1**.

O'Reilly, J.A. (2019a) Event-related potential arithmetic to analyze offset potentials from conscious mice. *J. Neurosci. Methods*, **318**, 78–83.

O'Reilly, J.A. (2019b) Double-epoch subtraction reveals long-latency mismatch response in urethane-anaesthetized mice. *J. Neurosci. Methods*, **326**, 108375.

Pakarinen, S., Takegata, R., Rinne, T., Huotilainen, M., & Näätänen, R. (2007) Measurement of extensive auditory discrimination profiles using the mismatch negativity (MMN) of the auditory event-related potential (ERP). *Clin. Neurophysiol.*, **118**, 177–185.

Park, Y.-M., Lee, S.-H., Kim, S., & Bae, S.-M. (2010) The loudness dependence of the auditory evoked potential (LDAEP) in schizophrenia, bipolar disorder, major depressive disorder, anxiety disorder, and healthy controls. *Prog. Neuro-Psychopharmacology Biol. Psychiatry*, **34**, 313–316.

Parras, G.G., Nieto-Diego, J., Carbajal, G. V., Valdés-Baizabal, C., Escera, C., & Malmierca, M.S. (2017) Neurons along the auditory pathway exhibit a hierarchical organization of prediction error. *Nat. Commun.*, **8**, 2148.

Paxinos, G. & Franklin, K.B.J. (2004) *The Mouse Brain in Stereotaxic Coordinates*. Elsevier Academic Press.

Pazo-Alvarez, P., Cadaveira, F., & Amenedo, E. (2003) MMN in the visual modality: A review. *Biol. Psychol.*, **63**, 199–236.

Perrin, M.A., Kantrowitz, J.T., Silipo, G., Dias, E., Jabado, O., & Javitt, D.C. (2018) Mismatch negativity (MMN) to spatial deviants and behavioral spatial discrimination ability in the etiology of auditory verbal hallucinations and thought disorder in schizophrenia. *Schizophr. Res.*, **191**, 140–147.

Phillips, D.P., Hall, S.E., & Boehnke, S.E. (2002) Central auditory onset responses, and temporal asymmetries in auditory perception. *Hear. Res.*, **167**, 192–205.

Phillips, D.P. & Irvine, D.R.F. (1981) Responses of single neurons in physiologically defined primary auditory cortex (AI) of the cat: Frequency tuning and responses to intensity. *J. Neurophysiol.*, **45**, 48–58.

Picton, T.W., Hillyard, S.A., & Galambos, R. (1976) Habituation and Attention in the Auditory System. In *Auditory System*. pp. 343–389.

Picton, T.W., Woods, D.L., Baribeau-Braun, J., & Healey, T.M.G. (1977) Evoked potential audiometry. *J Otolaryngol*, **6**, 90–119.

Polterovich, A., Jankowski, M.M., & Nelken, I. (2018) Deviance sensitivity in the auditory cortex of freely moving rats. *PLoS One*, **13**, e0197678.

Qin, L., Chimoto, S., Sakai, M., Wang, J.Y., & Sato, Y. (2007) Comparison between offset and onset responses of primary auditory cortex ON-OFF neurons in awake cats. *J. Neurophysiol.*, **97**, 3421–3431.

Rosburg, T. (2003) Left hemispheric dipole locations of the neuromagnetic mismatch negativity to frequency, intensity and duration deviants. *Cogn. Brain Res.*, **16**, 83–90.

Ross, J.M. & Hamm, J.P. (2020) Cortical Microcircuit Mechanisms of Mismatch Negativity and Its Underlying Subcomponents. *Front. Neural Circuits*, **14**, 13.

RStudio Team (2016) RStudio: Integrated Development Environment for R.

Ruusuvirta, T., Lipponen, A., Pellinen, E., Penttonen, M., & Astikainen, P. (2013) Auditory Cortical and Hippocampal-System Mismatch Responses to Duration Deviants in Urethane-Anesthetized Rats. *PLoS One*, **8**, e54624.

Ruusuvirta, T., Lipponen, A., Pellinen, E.K., Penttonen, M., & Astikainen, P. (2015) Auditory cortical and hippocampal local-field potentials to frequency deviant tones in urethane-anesthetized rats: An unexpected role of the sound frequencies themselves. *Int. J. Psychophysiol.*, **96**, 134–140.

Sakata, S. & Harris, K.D. (2009) Laminar structure of spontaneous and sensory-evoked population activity in auditory cortex. *Neuron*, **64**, 404–418.

Scholl, B., Gao, X., & Wehr, M. (2010) Nonoverlapping sets of synapses drive on responses and off responses in auditory cortex. *Neuron*, **65**, 412–421.

Schröger, E. & Wolff, C. (1996) Mismatch response of the human brain to changes in sound location. *Neuroreport*, **7**, 3005–3008.

Shelley, A.M., Ward, P.B., Catts, S. V, Michie, P.T., Andrews, S., & McConaghy, N. (1991) Mismatch negativity: An index of a preattentive processing deficit in schizophrenia. *Biol. Psychiatry*, **30**, 1059–1062.

Shen, G., Smyk, N.J., Meltzoff, A.N., & Marshall, P.J. (2018) Using somatosensory mismatch responses as a window into somatotopic processing of tactile stimulation. *Psychophysiology*, **55**, e13030.

Shiramatsu, T.I., Kanzaki, R., & Takahashi, H. (2013) Cortical mapping of mismatch negativity with deviance detection property in rat. *PLoS One*, **8**, e82663.

Siegel, S.J., Connolly, P., Liang, Y., Lenox, R.H., Gur, R.E., Bilker, W.B., Kanes, S.J., & Turetsky, B.I. (2003) Effects of strain, novelty, and NMDA blockade on auditory-evoked potentials in mice. *Neuropsychopharmacology*, **28**, 675–682.

Sivarao, D. V., Chen, P., Yang, Y., Li, Y.W., Pieschl, R., & Ahlijanian K., M.K. (2014) NR2B antagonist CP-101,606 abolishes pitch-mediated deviance detection in

awake rats. *Front. Psychiatry*, **5**, 96.

Takahashi, H., Nakao, M., & Kaga, K. (2004) Cortical mapping of auditory-evoked offset responses in rats. *Neuroreport*, **15**, 1565–1569.

Takegata, R., Tervaniemi, M., Alku, P., Ylinen, S., & Näätänen, R. (2008) Parameter-specific modulation of the mismatch negativity to duration decrement and increment: Evidence for asymmetric processes. *Clin. Neurophysiol.*, **119**, 1515–1523.

Todd, J., Michie, P.T., Schall, U., Karayanidis, F., Yabe, H., & Näätänen, R. (2008) Deviant matters: Duration, frequency, and intensity deviants reveal different patterns of mismatch negativity reduction in early and late schizophrenia. *Biol. Psychiatry*, **63**, 58–64.

Ulanovsky, N., Las, L., Farkas, D., & Nelken, I. (2004) Multiple time scales of adaptation in auditory cortex neurons. *J. Neurosci.*, **24**, 10440–10453.

Ulanovsky, N., Las, L., & Nelken, I. (2003) Processing of low-probability sounds by cortical neurons. *Nat. Neurosci.*, **6**, 391–398.

Umbricht, D. & Krljes, S. (2005) Mismatch negativity in schizophrenia: a meta-analysis. *Schizophr. Res.*, **76**, 1–23.

Umbricht, D., Vyssotki, D., Latanov, A., Nitsch, R., & Lipp, H.P. (2005) Deviance-related electrophysiological activity in mice: Is there mismatch negativity in mice? *Clin. Neurophysiol.*, **116**, 353–363.

Wacongne, C., Changeux, J.P., & Dehaene, S. (2012) A neuronal model of predictive coding accounting for the mismatch negativity. *J. Neurosci.*, **32**, 3665–3678.

Wiens, S., Szychowska, M., Eklund, R., & van Berlekom, E. (2019) Cascade and no-repetition rules are comparable controls for the auditory frequency mismatch negativity in oddball tasks. *Psychophysiology*, **56**, e13280.

Winkler, I., Karmos, G., & Näätänen, R. (1996) Adaptive modeling of the unattended acoustic environment reflected in the mismatch negativity event-related potential. *Brain Res.*, **742**, 239–252.

Yamashiro, K., Inui, K., Otsuru, N., Kida, T., & Kakigi, R. (2009) Automatic auditory off-response in humans: An MEG study. *Eur. J. Neurosci.*, **30**, 125–131.

Figure Captions

Figure 1: Overview of difference waveform computations. a) The oddball paradigm and many-standard control sequences were presented in consecutive blocks. b) Simplified illustration of the effects observed on auditory evoked potentials. c) Difference waveform computations, summarising key observations. These analyses were designed to identify any differences between standard, oddball, and control conditions; however, the results were interpreted to reflect physical sensitivity and habituation of the auditory response.

Figure 2: AEP waveforms from many-standards control paradigms. Grand-averages from urethane-anaesthetised mice in duration (a), frequency (b), and intensity (c) varying paradigms are plotted in the left panel. Grand-averages from conscious mice in duration (d), frequency (e), intensity (f), and ISI (g) paradigms are plotted in the right panel. Three AEP components are identified: a negative amplitude onset response (N1), positive amplitude onset response (P1; conscious group only), and positive amplitude offset response (P_{off}). Note the different y-axis scales in left and right panels, and different x-axis scales in duration-varying paradigms (a) and (d).

Figure 3: AEP measurements from many-standards control paradigms. Data from the anaesthetised cohort (left) includes the effects of stimulus duration on N1 peak amplitude and P_{off} peak latency (a), and frequency (b) and intensity (c) on N1 and P_{off} peak amplitudes. Data from the conscious cohort (right) includes the effects of stimulus frequency (d), intensity (e), and inter-stimulus interval (f) on N1 and P1 peak amplitudes. All of these relationships were found to be statistically significant, with the exception of stimulus duration and N1 peak amplitude. Means ± SEM are shown with black and grey horizontal bars.

Figure 4: AEP, classical MMR, and controlled MMR waveforms from urethane-anaesthetised mice in response to duration (a), frequency (b), and intensity (c) deviance. Standard (STD_{OD}), oddball (DEV_{OD}) and control (DEV_{CTR} and STD_{CTR}) stimuli are identified in the key of each plot. Difference waveform amplitudes significantly above or below zero ($p < 0.05$; FDR-corrected) are denoted in MMR plots with solid bars coloured to match the corresponding OD waveform; this can only be observed from classical duration MMR waveforms. Note the different timescale for duration-varying waveforms in (a); shaded regions represent SEM.

Figure 5: AEP, classical MMR, and controlled MMR waveforms from conscious mice in response to duration (a), frequency (b), intensity (c), and ISI (d) deviance. Standard (STD_{OD}), oddball (DEV_{OD}) and control (DEV_{CTR} and STD_{CTR}) stimuli are labelled in the respective keys of each plot. None of these difference waveforms achieved the threshold for statistical significance with FDR correction. Note the different x-axis scales used for AEP and MMR waveforms; different y-axis scales for duration-varying waveforms in (a); shaded regions represent SEM.

Figure 6: AEP peak measurement data from oddball and many-standards control paradigms. Data from the anaesthetised group (left) includes N1 and Poff peak amplitudes from different duration (a), frequency (b), and intensity (c) stimuli presented as standard (STD) and deviant (DEV) in oddball (OD) and many-standards control (CTR) paradigms. Data from the conscious cohort (right) includes N1 and P1 peak amplitudes from duration (d), frequency (e), intensity (f) and inter-stimulus interval (g). Means ± SEM are shown with black and grey horizontal bars.

Supplementary Information

1. Auditory-evoked potential changes in anaesthetised mice

The urethane-anaesthetised cohort was presented with oddball and control paradigms in a fixed sequence, as shown in Figure S1. Each stimulus block included presentation of a 100 ms, 10 kHz, 80 dBA stimulus, with a 450 ms inter-stimulus interval; identified as the "standard" in oddball paradigms, but also included in all of the many-standards control paradigms. This facilitated an examination of the influence of deepening anaesthesia and repeated auditory stimulation throughout the course of this experiment. Peak amplitude measurements (N1 and P_{off}) from these identical stimuli presented in different stimulus blocks are plotted in Figure S2. Repeated measures ANOVA with stimulus block as a within-subjects factor revealed a significant effect of stimulus block on N1 [$F_{5,65}$ = 8.63, p = .0006; Greenhouse–Geisser correction, ε = .47], but not P_{off} [$F_{5,65}$ = 2.18, p = .117; Greenhouse–Geisser correction, ε = .52] peak amplitudes. Although urethane is considered to be a relatively stable anaesthetic (Lee & Jones, 2018), without data related specifically to anaesthetic state it is impossible to establish whether this effect is predominantly influenced by auditory habituation, anaesthetic state, or some other factor(s).

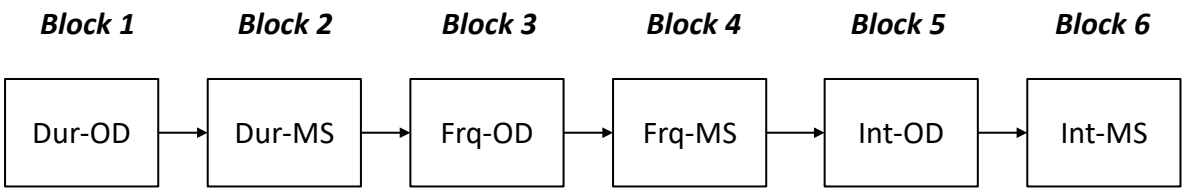

Figure S1: Stimulus blocks presented to urethane-anaesthetised mice. This sequence was fixed for all animals in this cohort. Duration (Dur), frequency (Frq) and intensity (Int) of stimuli was varied in oddball (OD) and many-standards (MS) paradigms.

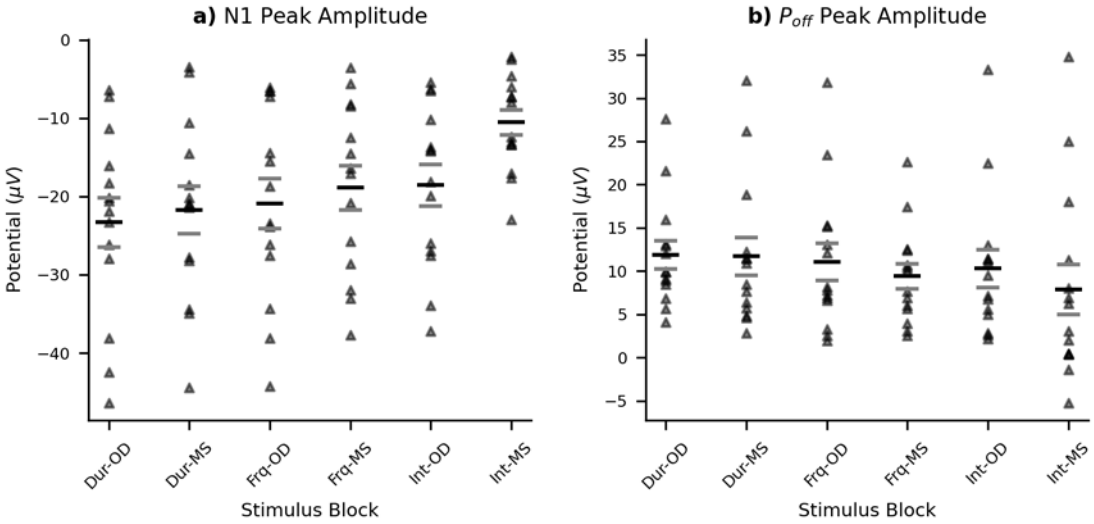

Figure S2: AEP peak amplitudes from the same stimuli presented in different blocks. a) N1 amplitude. b) P_{off} amplitude. In each block, the eliciting stimulus was a 100 ms, 10 kHz, 80 dBA pure-tone sinusoid, preceded by a 450 ms ISI; however, it must be noted that the context(s) varied considerably. Mean ± SEM are shown with black and grey horizontal bars, respectively. Offset response peak amplitude was quantified with 10 ms pre-stimulus-offset average baseline correction.

2. Effect of sound level measurement weightings

The sound meter used to calibrate stimuli applied A-weightings, which imposes a non-linear frequency-intensity relationship. This is designed to account for human hearing sensitivity, which is non-linear across the pressure wave spectrum; however, inadvertently introduces confounds for interpretation of the effects of stimulus frequency on AEP waveforms. Animals also exhibit non-linear hearing sensitivity to tone frequency (Turner *et al.*, 2005). This compounded non-linearity of frequency loudness perception and sound calibration presents a complex and challenging issue to deal with in cross-species auditory neurophysiology research. An argument may be made that the effects of stimulus frequency observed in the present study reflect changes in intensity due to sound level weighting during calibration.

This hypothesis may be evaluated by analysing data from frequency many-standards paradigms presented to urethane-anaesthetised (Table S1 and Figure S3a) and conscious mice (Table S2 and Figure S3b-d). It can be seen from Table S1 that 1.25 kHz and 5 kHz stimuli have approximately equal weighting applied, producing an absolute SPL for both frequencies of 79.4 dB; however there is a significant difference between their resulting N1 peak amplitudes [t_{13} = 3.134, p = .0079; two-sided dependent t-test], as shown in Figure S3a. This demonstrates that stimulus frequency influences changes in N1 peak amplitude in urethane-anaesthetised mice, rather than these changes simply reflecting intensity differences.

In contrast, the range of frequencies employed in the many-standards control paradigm presented to conscious animals did not include any different frequency stimuli with the same absolute SPL. Nevertheless, it is possible to examine the influence of stimulus frequency and intensity by comparing data from both frequency and intensity many-standards control paradigms. Figure S3b shows N1 peak amplitudes (mean ± SEM) from these paradigms, plotted by absolute stimulus intensity. Lines fit by least squares linear regression indicate that the effect of frequency (slope = −7.228) is different from that of intensity (slope = −1.295). Lines fit to N1 peak amplitude measurements from individual conscious animals are shown in Figure S3c. Statistical analysis of this data revealed a significant difference between frequency-varying and intensity-varying stimuli [t_{19} = −2.895, p = .0093; two-sided dependent t-test], as illustrated in Figure S3d. This suggests that modulation of N1 peak amplitudes by stimulus frequency is not merely a side effect of non-linear sound level calibration; in agreement with established knowledge (Picton *et al.*, 1977). To avoid such confounds in future studies, it is recommended to use Z(zero)-weightings for SPL calibration; although non-linear tone loudness perception will

remain a complex and challenging issue to address in cross-species auditory neurophysiology research.

Table S1: Sound levels of different frequency stimuli presented in frequency many-standards paradigm to urethane-anaesthetised mice.

Frequency (kHz)	A-weighting	dBA	dB	N1 Peak (μV)
1.25	0.576	80	79.4	−6.280 ± 1.516
2.50	1.271	80	78.7	−7.618 ± 1.515
3.75	1.047	80	78.9	−8.016 ±1.866
5.00	0.556	80	79.4	−11.864 ± 2.841
6.25	−0.086	80	80.1	−10.525 ± 1.643
7.50	−0.827	80	80.8	−14.203 ± 2.374
8.75	−1.636	80	81.6	−17.237 ± 3.091
10.00	−2.488	80	82.5	−18.868 ± 2.944
11.25	−3.364	80	82.4	−22.384 ± 3.046
12.50	−4.250	80	84.2	−22.850 ± 3.580

N1 peak amplitudes are reported as mean ± SEM

Table S2: Sound levels of different frequency stimuli presented in frequency many-standards paradigm to conscious mice.

Frequency (kHz)	A-weighting	dBA	dB	N1 Peak (μV)
8.0	−1.144	80	81.1	−23.557 ± 3.367
8.5	−1.470	80	81.5	−29.963 ± 4.095
9.0	−1.804	80	81.8	−33.783 ± 3.928
9.5	−2.144	80	82.1	−31.864 ± 3.655
10.0	−2.488	80	82.5	−34.905 ± 5.143
10.5	−2.837	80	82.8	−33.331 ± 5.078
11.0	−3.188	80	83.2	−43.814 ± 5.250
11.5	−3.541	80	83.5	−47.305 ± 5.459
12.0	−3.895	80	83.9	−44.165 ± 5.579
12.5	−4.250	80	84.2	−46.871 ± 4.881

N1 peak amplitudes are reported as mean ± SEM

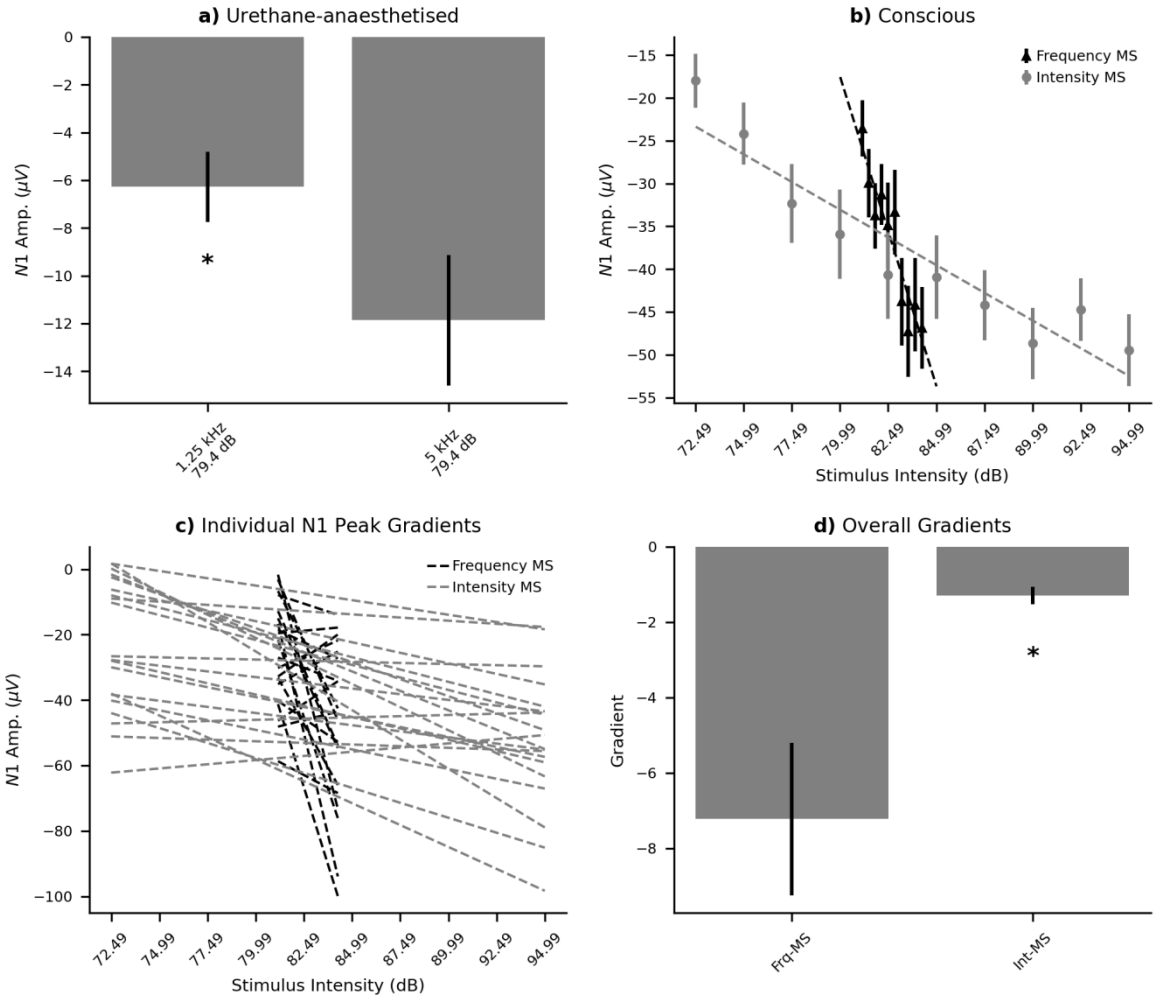

Figure S3: Analysis of the potential impact of A-weighting applied to sound level calibration. In urethane-anaesthetised mice two different frequency stimuli with the same absolute SPL elicit significantly different N1 peak amplitudes (a). Mean N1 peak amplitudes from conscious mice in frequency and intensity many-standards (MS) paradigms, plotted by absolute SPL (b). Gradients associated with N1 peak amplitude measurements from frequency and intensity MS paradigms from each animal, plotted by absolute SPL. Comparison of mean N1 peak amplitude gradients from (c) is shown in (d). Bar charts show mean ± SEM; dashed lines in (b) portray least-squares fit; asterisks represent $p < .05$ in a two-sided dependent t-test.

References

Lee, C. & Jones, T.A. (2018) Effects of ketamine compared with urethane anesthesia on vestibular sensory evoked potentials and systemic physiology in mice. *J. Am. Assoc. Lab. Anim. Sci.*, **57**, 268–277.

Picton, T.W., Woods, D.L., Baribeau-Braun, J., & Healey, T.M.G. (1977) Evoked potential audiometry. *J Otolaryngol*, **6**, 90–119.

Turner, J.G., Parrish, J.L., Hughes, L.F., Toth, L.A., & Caspary, D.M. (2005) Hearing in laboratory animals: Strain differences and nonauditory effects of noise. *Comp. Med.*, **55**, 12–23.

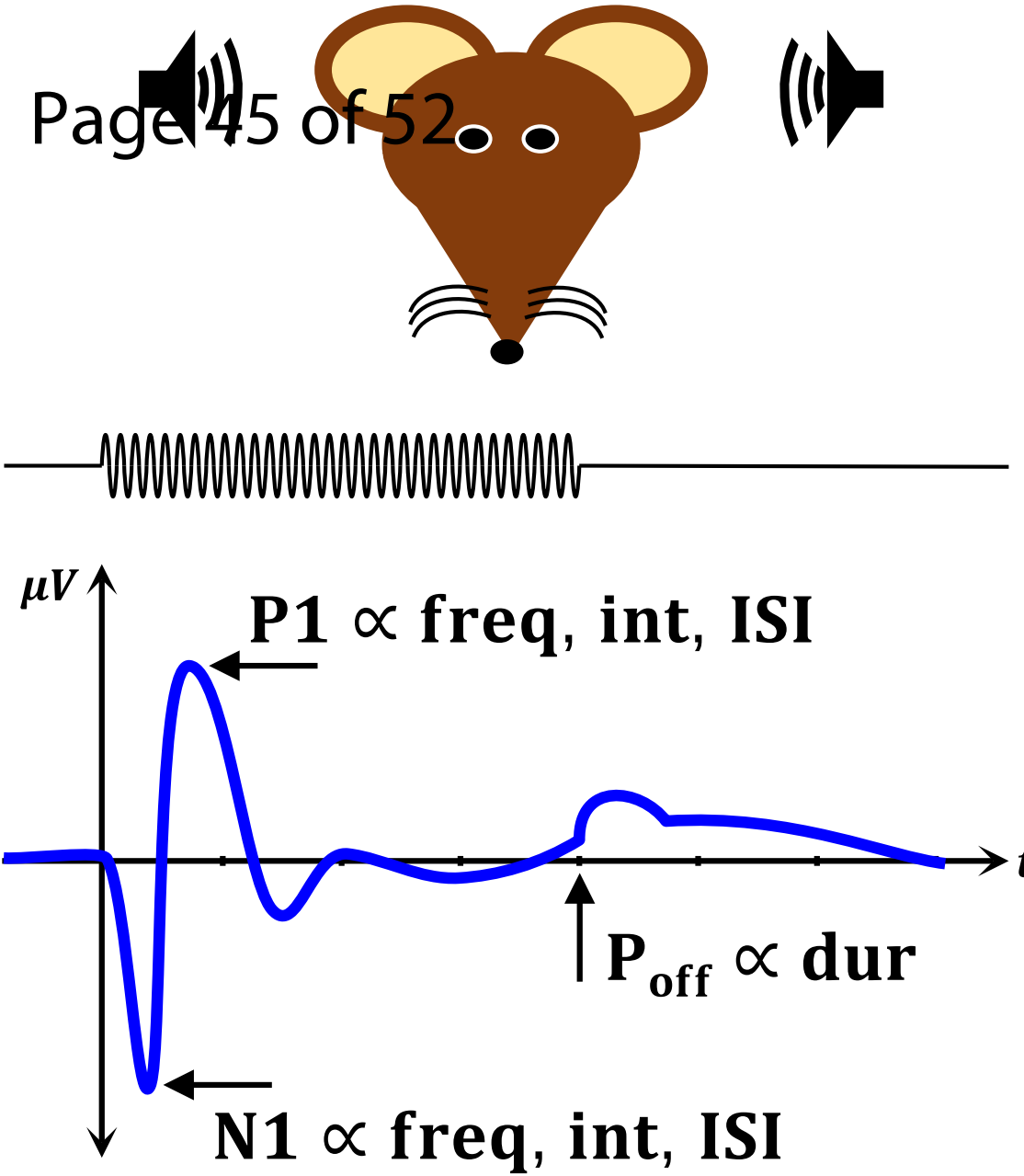
μV
P1 ∝ freq, int, ISI
t
P_off ∝ dur
N1 ∝ freq, int, ISI

Stimulus duration correlated with stimulus-off response peak latency. Frequency, intensity, and inter-stimulus interval correlated with stimulus-on N1 and P1 (conscious only) peak amplitudes. These relationships were instrumental in shaping classical MMR morphology, reflecting modification of normal auditory processing by different physical properties of sound. Controlled MMR waveforms exhibited auditory habituation, equally observed in both *oddball* and *standard* conditions.

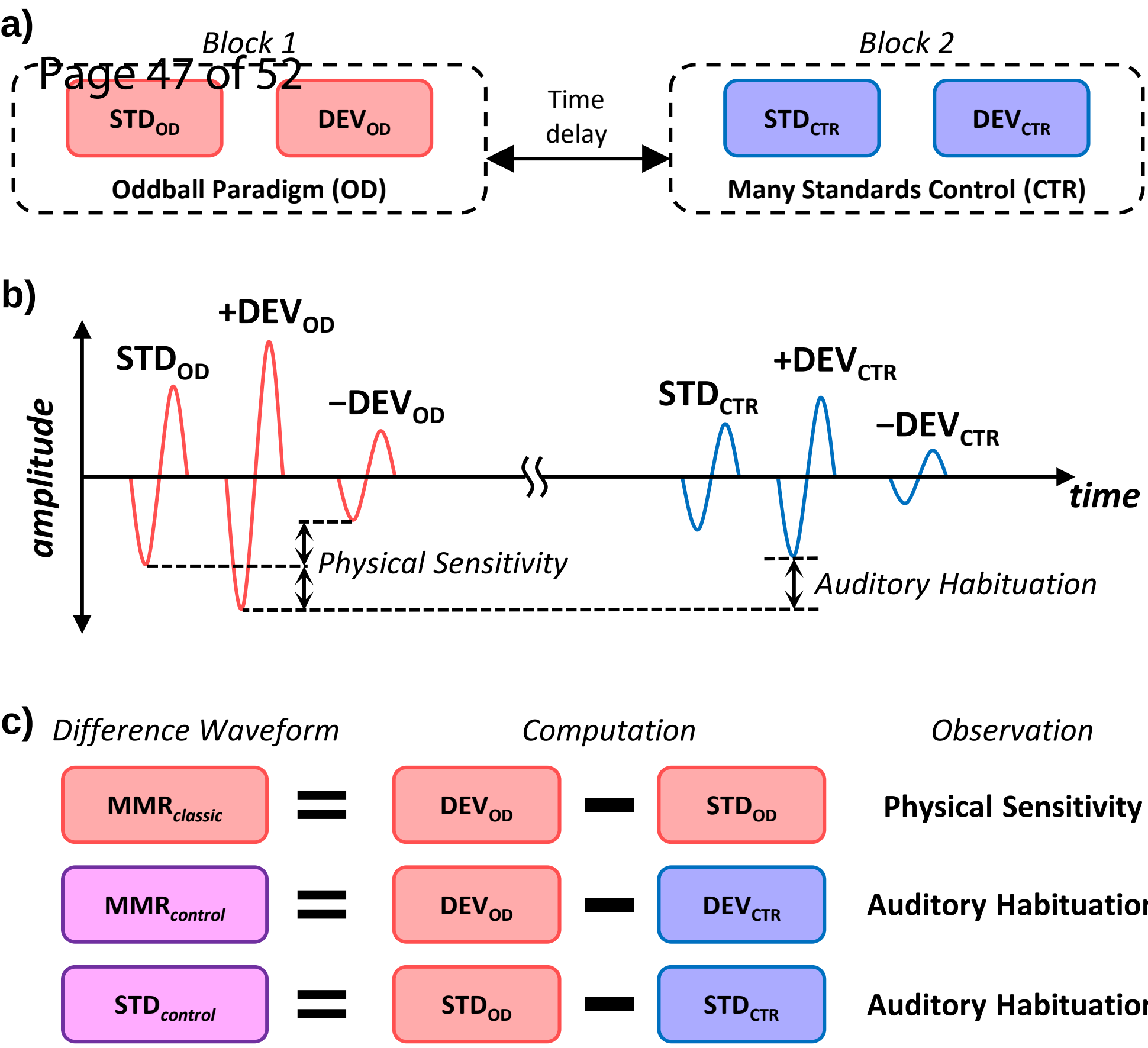
a)
Block 1
STD_OD
DEV_OD
Oddball Paradigm (OD)
Time delay
Block 2
STD_CTR
DEV_CTR
Many Standards Control (CTR)
b)
+DEV_OD
STD_OD
–DEV_OD
+DEV_CTR
STD_CTR
–DEV_CTR
amplitude
time
Physical Sensitivity
Auditory Habituation
c)
Difference Waveform
Computation
Observation
MMR_classic = DEV_OD – STD_OD
Physical Sensitivity
MMR_control = DEV_OD – DEV_CTR
Auditory Habituation
STD_control = STD_OD – STD_CTR
Auditory Habituation

Anaesthetised

Conscious

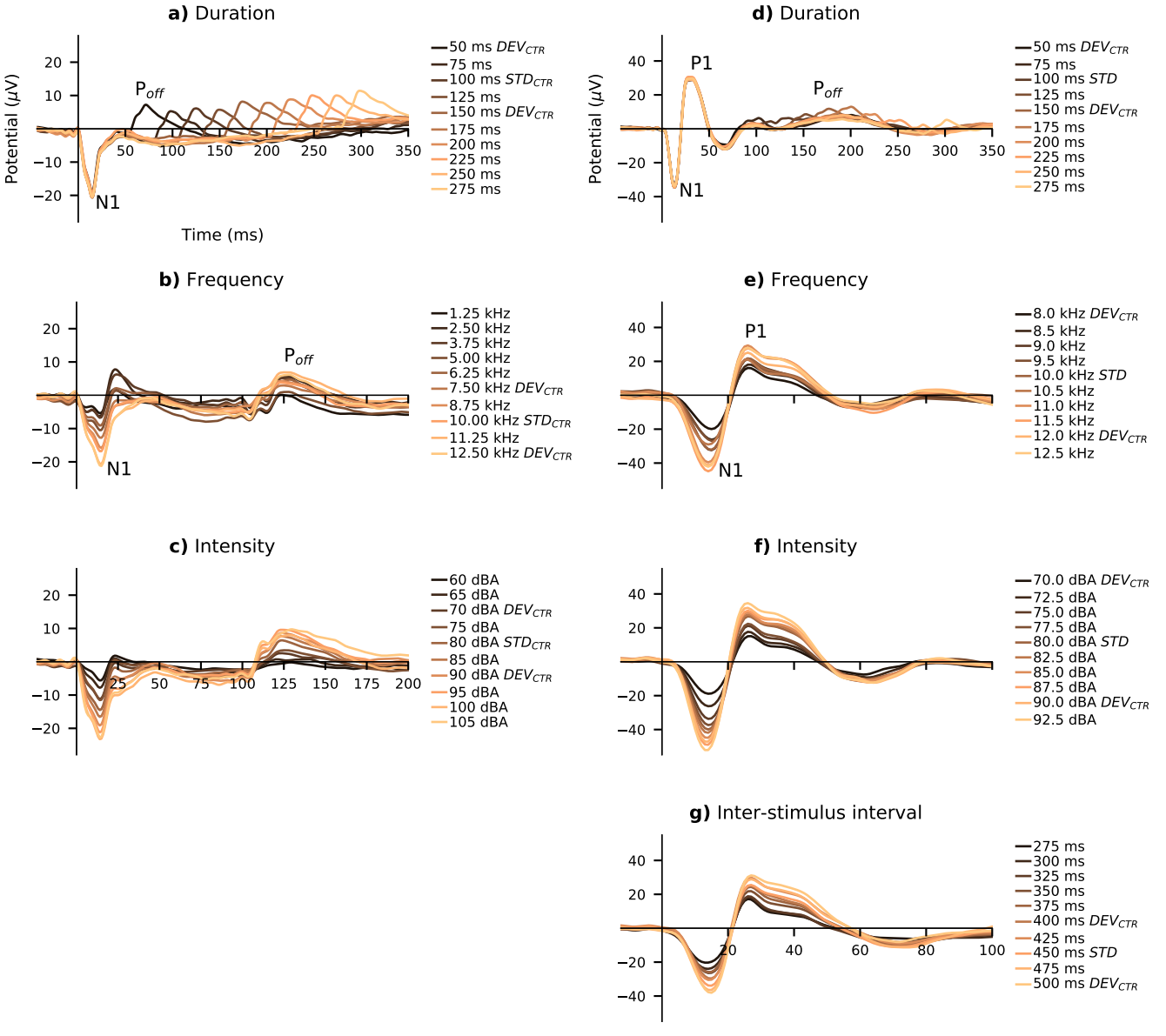

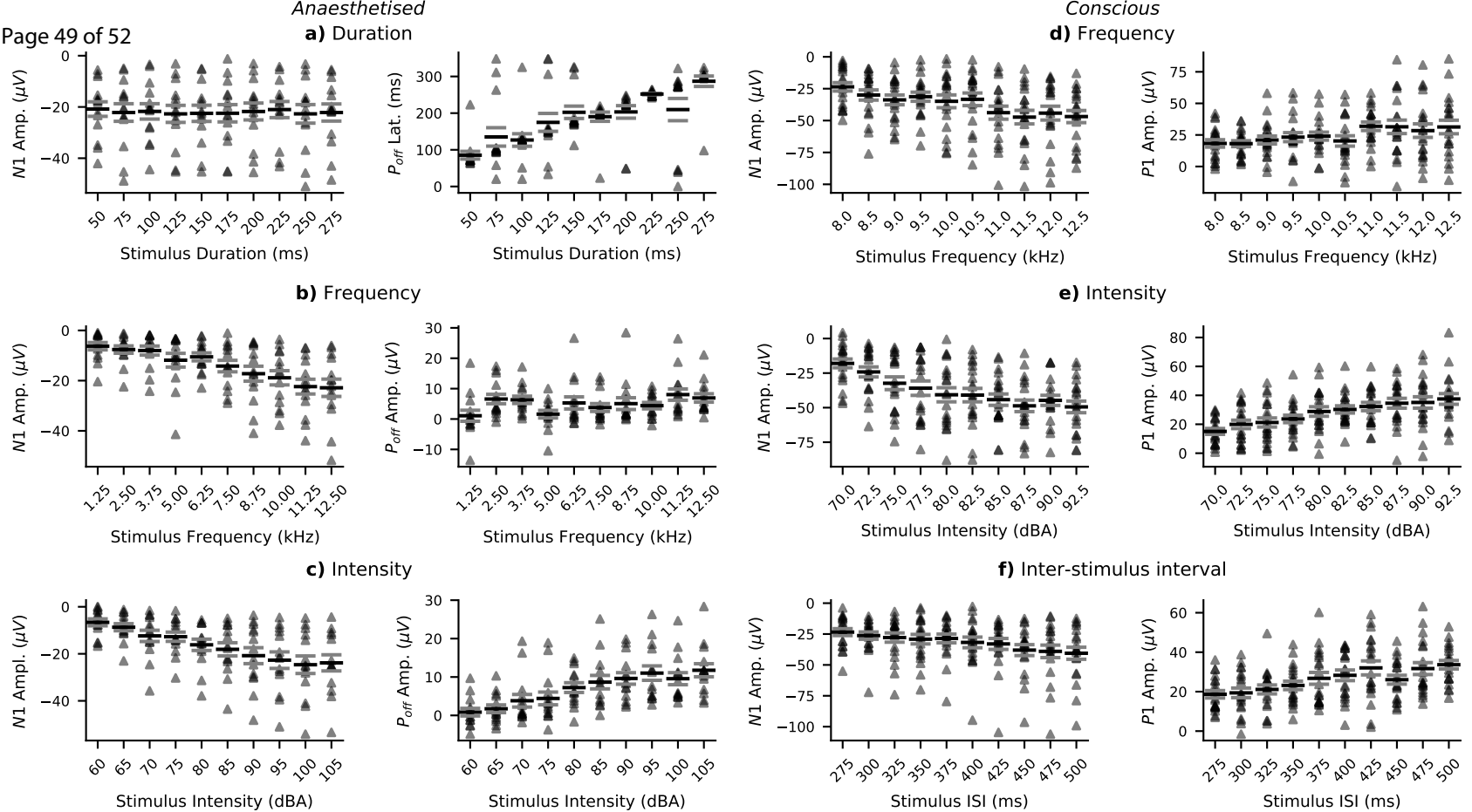
Anaesthetised
Conscious
a) Duration
d) Frequency
b) Frequency
e) Intensity
c) Intensity
f) Inter-stimulus interval
N1 Amp. (μV)
N1 Ampl. (μV)
P_off Lat. (ms)
P_off Amp. (μV)
P1 Amp. (μV)
Stimulus Duration (ms)
Stimulus Frequency (kHz)
Stimulus Intensity (dBA)
Stimulus ISI (ms)

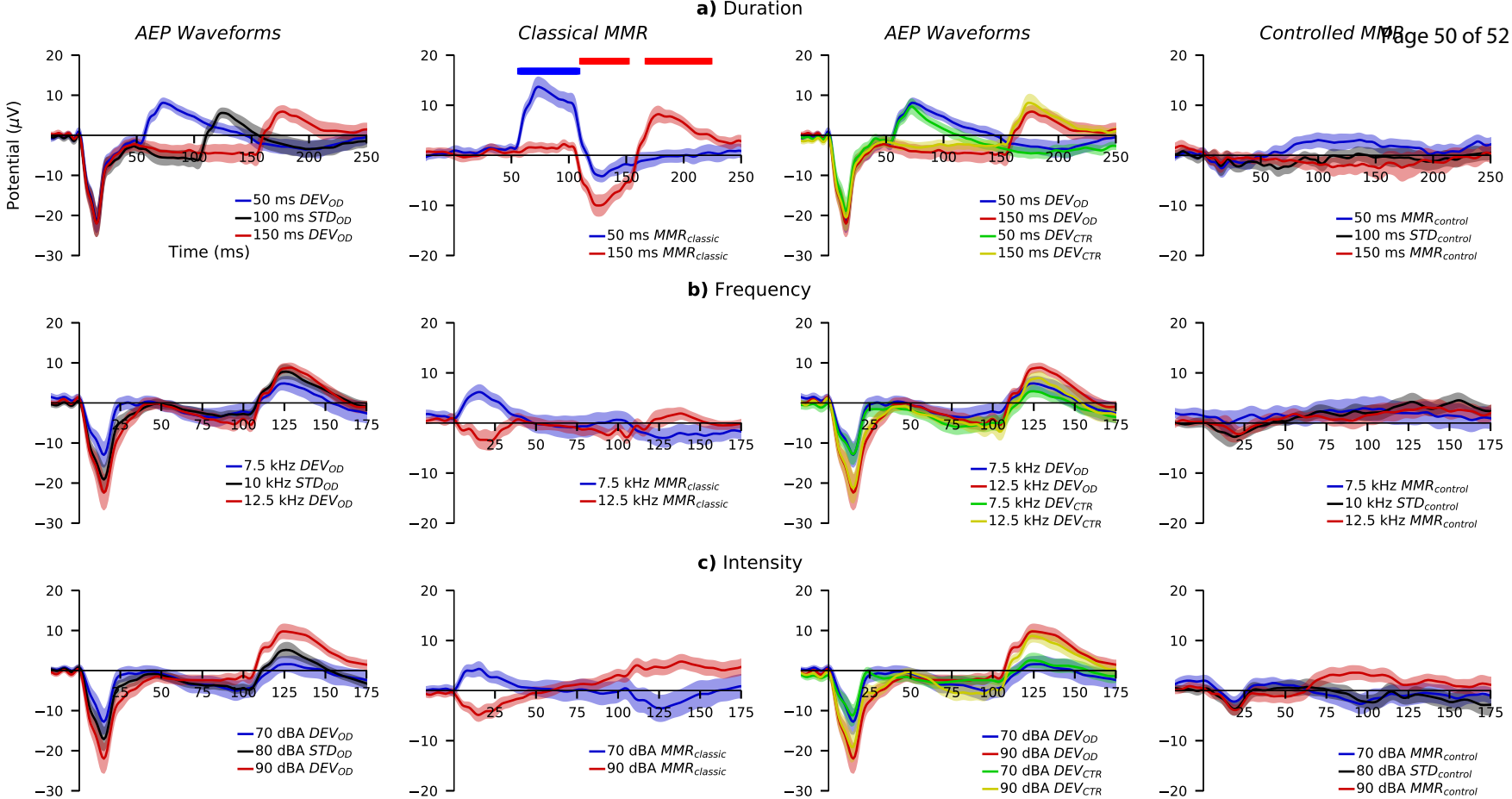
a) Duration
AEP Waveforms
Classical MMR
AEP Waveforms
Controlled MMR
Potential (μV)
Time (ms)
50 ms DEV_OD
100 ms STD_OD
150 ms DEV_OD
50 ms MMR_classic
150 ms MMR_classic
50 ms DEV_OD
150 ms DEV_OD
50 ms DEV_CTR
150 ms DEV_CTR
50 ms MMR_control
100 ms STD_control
150 ms MMR_control
b) Frequency
7.5 kHz DEV_OD
10 kHz STD_OD
12.5 kHz DEV_OD
7.5 kHz MMR_classic
12.5 kHz MMR_classic
7.5 kHz DEV_OD
12.5 kHz DEV_OD
7.5 kHz DEV_CTR
12.5 kHz DEV_CTR
7.5 kHz MMR_control
10 kHz STD_control
12.5 kHz MMR_control
c) Intensity
70 dBA DEV_OD
80 dBA STD_OD
90 dBA DEV_OD
70 dBA MMR_classic
90 dBA MMR_classic
70 dBA DEV_OD
90 dBA DEV_OD
70 dBA DEV_CTR
90 dBA DEV_CTR
70 dBA MMR_control
80 dBA STD_control
90 dBA MMR_control

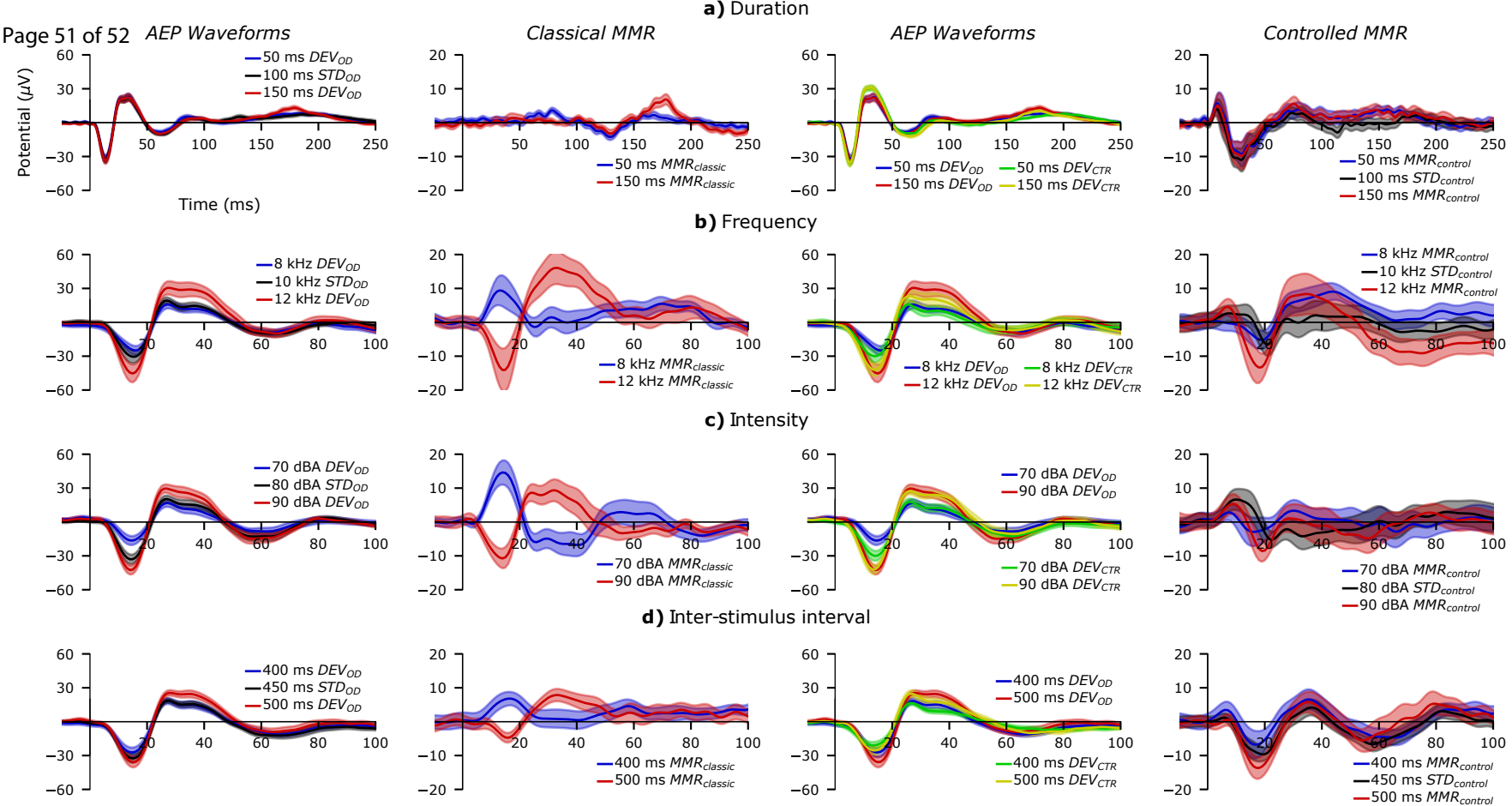
a) Duration
AEP Waveforms
Classical MMR
AEP Waveforms
Controlled MMR
Potential (μV)
Time (ms)
50 ms DEV_OD
100 ms STD_OD
150 ms DEV_OD
50 ms MMR_classic
150 ms MMR_classic
50 ms DEV_OD
50 ms DEV_CTR
150 ms DEV_OD
150 ms DEV_CTR
50 ms MMR_control
100 ms STD_control
150 ms MMR_control
b) Frequency
8 kHz DEV_OD
10 kHz STD_OD
12 kHz DEV_OD
8 kHz MMR_classic
12 kHz MMR_classic
8 kHz DEV_OD
8 kHz DEV_CTR
12 kHz DEV_OD
12 kHz DEV_CTR
8 kHz MMR_control
10 kHz STD_control
12 kHz MMR_control
c) Intensity
70 dBA DEV_OD
80 dBA STD_OD
90 dBA DEV_OD
70 dBA MMR_classic
90 dBA MMR_classic
70 dBA DEV_OD
90 dBA DEV_OD
70 dBA DEV_CTR
90 dBA DEV_CTR
70 dBA MMR_control
80 dBA STD_control
90 dBA MMR_control
d) Inter-stimulus interval
400 ms DEV_OD
450 ms STD_OD
500 ms DEV_OD
400 ms MMR_classic
500 ms MMR_classic
400 ms DEV_OD
500 ms DEV_OD
400 ms DEV_CTR
500 ms DEV_CTR
400 ms MMR_control
450 ms STD_control
500 ms MMR_control

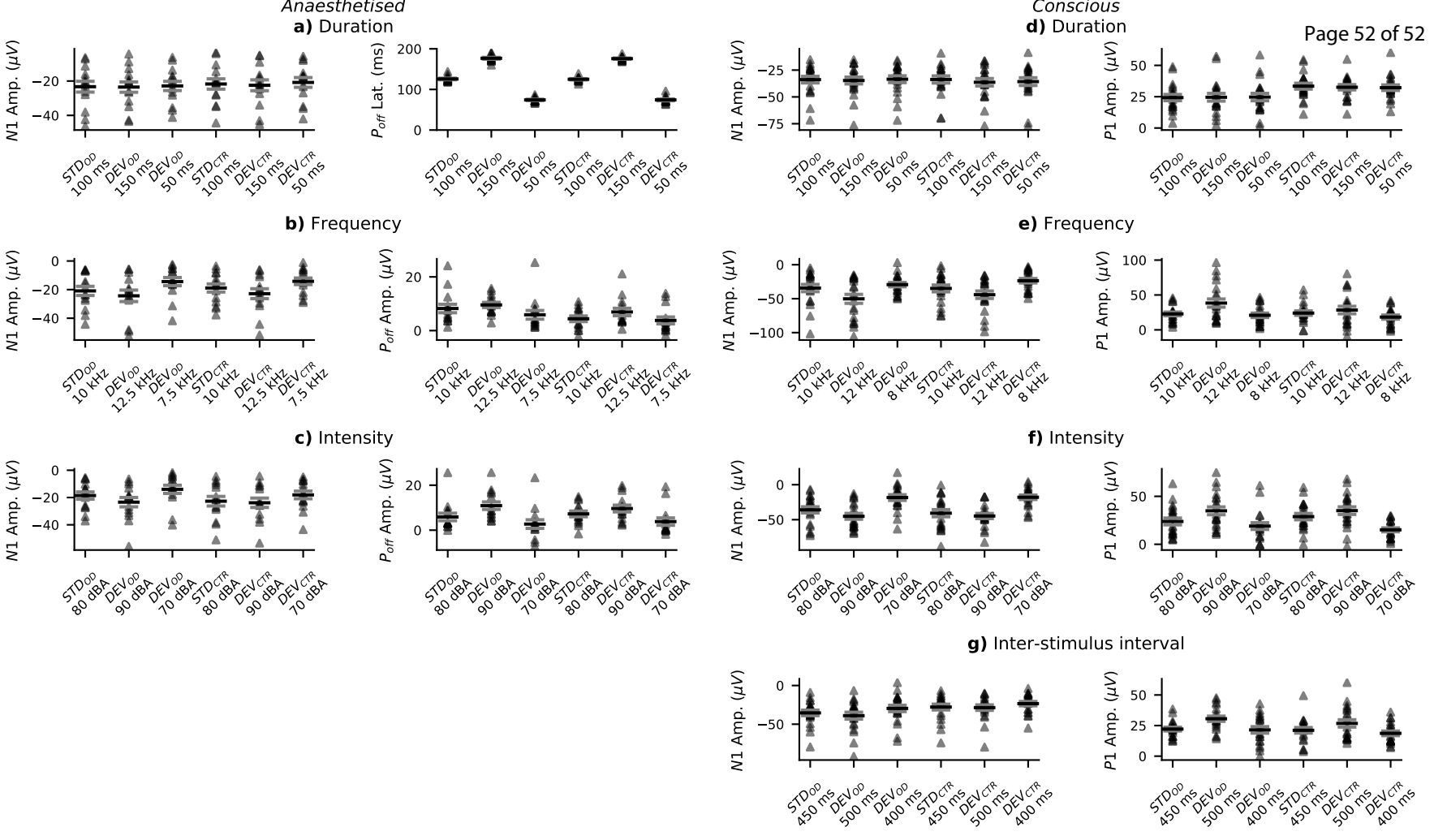
Anaesthetised
Conscious
a) Duration
b) Frequency
c) Intensity
d) Duration
e) Frequency
f) Intensity
g) Inter-stimulus interval
N1 Amp. (μV)
P1 Amp. (μV)
Poff Lat. (ms)
Poff Amp. (μV)
STDOD 100 ms
DEVOD 150 ms
DEVOD 50 ms
STDCTR 100 ms
DEVCTR 150 ms
DEVCTR 50 ms
STDOD 10 kHz
DEVOD 12.5 kHz
DEVOD 7.5 kHz
STDCTR 10 kHz
DEVCTR 12.5 kHz
DEVCTR 7.5 kHz
STDOD 80 dBA
DEVOD 90 dBA
DEVOD 70 dBA
STDCTR 80 dBA
DEVCTR 90 dBA
DEVCTR 70 dBA
STDOD 10 kHz
DEVOD 12 kHz
DEVOD 8 kHz
STDCTR 10 kHz
DEVCTR 12 kHz
DEVCTR 8 kHz
STDOD 450 ms
DEVOD 500 ms
DEVOD 400 ms
STDCTR 450 ms
DEVCTR 500 ms
DEVCTR 400 ms